IEEE Access
Multidisciplinary | Rapid Review | Open Access Journal

Received May 25, 2022, accepted June 6, 2022, date of publication June 13, 2022, date of current version June 17, 2022.

*Digital Object Identifier 10.1109/ACCESS.2022.3182875*

# Hunting Based Optimization Techniques Used in Controlling an Active Magnetic Bearing System

**SURAJ GUPTA[1], PABITRA KUMAR BISWAS[1], (Member, IEEE), THANIKANTI SUDHAKAR BABU[2], (Senior Member, IEEE), AND HASSAN HAES ALHELOU[3], (Senior Member, IEEE)**

[1]National Institute of Technology Mizoram, Aizawl 796012, India
[2]Department of Electrical and Electronics Engineering, Chaitanya Bharathi Institute of Technology, Hyderabad 500075, India
[3]Department of Electrical Power Engineering, Faculty of Mechanical and Electrical Engineering, Tishreen University, Latakia 2230, Syria

Corresponding author: Hassan Haes Alhelou (alhelou@ieee.org) and Thanikanti Sudhakar Babu (sudhakarbabu66@gmail.com)

**ABSTRACT** This paper proposes a closed-loop and implements some metaheuristic optimization approaches to regulate an unstable active magnetic bearing (AMB) system. First of all, a hardware model of an AMB is fabricated in the laboratory. Mathematical analysis is carried out and a linearized open-loop transfer function is obtained for an equilibrium point of operation, using the parameters of the hardware model. Then, a closed loop is proposed for this AMB system, which comprises a PID controller, power amplifier, and position sensor. Further, three different metaheuristic nature-inspired hunting-based optimization algorithms i.e., Ant lion optimization (ALO), Grey wolf optimization (GWO), and Whale optimization algorithm (WOA) are implemented individually to calculate the gain parameters of the PID controller. Separately, the performance of these optimization algorithms is evaluated and observed on four different performance indices: integral of absolute error (IAE), integral of squared error (ISE), and an integral of time multiplied absolute error (ITAE) and integral of time multiplied squared error (ITSE). For a stable, efficient, and reliable bearing operation, it is vital to perform an analysis of the performance of optimization techniques with different objective functions for the proposed system. Therefore, few comparisons are conducted, first based on data obtained from statistical analysis. The second is based on data obtained from transient state performance and phase margin. Third on the scale of algorithm execution time. Finally, with the assistance of observed data effectiveness of each optimization technique to control the proposed AMB system is concluded which can serve as theoretical and experimental foundations for the continued use of AMB in high-speed applications.

**INDEX TERMS** Active magnetic bearing, metaheuristic, nature-inspired hunting-based algorithms, Ant lion optimization, Grey wolf optimization, Whale optimization algorithm.

## I. INTRODUCTION

Active magnetic bearings (AMBs) [1] are very popular because of their very high rotational speed, zero friction, high precision, fewer vibrations, longevity, low maintenance, ability to perform in high temperature and vacuum, etc [2]. Due to these advantageous characteristics, AMBs are highly demanding in many applications like satellite applications [3], machine tools [4], flywheel energy storage applications [5], marine rotor systems [6], and compressors [7] and in different other prominent areas [8].

It is evident from various research that active magnetic bearing is an inherently unstable system because of the non-linear relation between attractive force (coil current) and position of the rotor (air gap) [8]–[10]. As a result, a closed-loop control with a position controller must be designed to stabilize the rotor position at the nominal air gap. Numerous control strategies [10]–[16] have been proposed in literature but most of them are specific to their designed magnetic bearing model.

Among the available controlling techniques, PID is extensively used in the magnetic bearing control industry because it does not require a model and the controller design and debugging are untroublesome [17]. Mostly, in high-speed industrial operation, a conventional lead controller or a PID

The associate editor coordinating the review of this manuscript and approving it for publication was R. K. Saket.

controller is implemented [18]. These controllers employ a sufficient phase leading to the closed-loop bearing system such that the rotor position becomes stable. The problem associated with a conventional controller, especially a PID controller, is tuning the gain parameters [19] i.e., Proportional gain, integral gain, and derivative gain. An inappropriate combination of which can lead to unstable bearing operation. Other than this an improper value of derivative gain will lead to amplifying noise signal which results in more vibration in the system and hence required filters [20]. Therefore, to meet these varieties of standard for a closed-loop AMB system, a complex combination of conventional PID controller with a notch and low pass filter is required which results in a high order system transfer function and complicate the whole configuration [14].

To eliminate the use of complex additive circuits with PID controllers, values of gain parameters must be optimized in such a way that without disturbing the system stability the close loop performs well. In literature, different research and analysis have been carried out to rectify the aforesaid problems. In 2015, [19] C. Wei and D. Söffker, introduced a controller design for the AMB system using a nondominated sorting genetic algorithm [(NSGA-II), a variant of the multiobjective genetic algorithm (MOGA)]. In their work, an extended PID controller for two AMB systems is optimized with the NSGA-II optimization technique. In 2018 [21], J. Sun et. al. proposed a strategy to calculate PID gain parameters for a radial active magnetic bearing (RAMB) system based on the dynamic stiffness model and Routh-Hurwitz (RH) criterion. Later, A. Dhyani et. al., [22] implemented the moth flam optimization (MFO) technique to design a fuzzy-PID controller for an AMB system. In 2019, Y. Liu et. al., [23] calculated the gain parameters of a PID controller for eight-pole radial magnetic bearing using the variable-step fourth-order Runge–Kutta iteration method. Further, in 2021, S. Zhang et. al., [17] analyzed the dynamic behavior of PID controlled AMB system under the combined action of the Alford force.

Still many new metaheuristic optimization techniques are untouched which may optimize the gain parameters of a PID controller in a much more efficient way. Although there are various optimization techniques available in the literature [24] and feasibility of any optimization method can be observed only by implementing it. So, following the no free lunch theorem [25], the performance of some recently famous novel metaheuristic hunting based optimization algorithms i.e., ant lion optimization (ALO), grey wolf optimization (GWO), and whale optimization algorithm (WOA) have been analyzed to design a PID controller for the proposed closed-loop AMB system. A pictorial representation of the major contribution of the manuscript is depicted in Figure 1.

The main contribution of this research article is listed below-

1. A hardware model of an active magnetic bearing system is fabricated in a laboratory. This magnetic bearing has an electromagnet and a rotor (suspending object) which are made of iron having a relative permeability of 11000 and 5000 respectively. On the horizontal limb of the electromagnet, the copper winding is stacked which has a relative permeability of 0.88 and thickness of 17 SWG.

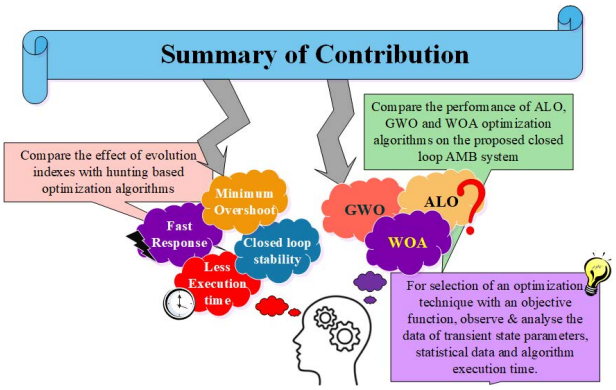


**FIGURE 1.** Major contributions of the manuscript.

2. After observing some set of experiments on the proposed system resistance and inductance value is calculated using and with the help of some mathematical analysis the proposed system is linearized at a nominal point of operation in a form of transfer function where the operating current ($i_o$) is 2.44 $A$ at an airgap ($x_o$) of 0.01 $m$.

3. Due to the instability of the open-loop AMB system, a closed-loop is proposed which comprises a PID controller, power amplifier, and a position sensor as a feedback path.

4. The gain values of the PID controller are calculated using three hunting-based optimization techniques which areant lion optimization, grey wolf optimization, and whale optimization algorithm. Each hunting algorithm is calibrated on the scale of four separate evaluation indexes i.e., integral of absolute error (IAE), integral of squared error (ISE), integral of time multiplied absolute error (ITAE) and integral of time multiplied squared error (ITSE).

5. To observe and analyze the performance of these optimization techniques several comparisons are carried out on the basis of statistical measures, closed-loop transient state performance including bode plot analysis, and time is taken in execution of the algorithm.

The remaining sections of this manuscript are organized as, Section 2 describes the modeling, analysis, and linearization of the hardware model of the proposed AMB system. Section 3 briefly explains three hunting-based optimization algorithms i.e., ALO, GWO, and WOA methods. Section 4 is the results and discussion which contains an implementation of this algorithm on the proposed AMB system and a comparison of their performances. Section 5 concludes the work.

## II. MODEL DESCRIPTION AND ANALYSIS OF ACTIVE MAGNETIC BEARING (AMB) SYSTEM

### A. HARDWARE MODEL DESCRIPTION

For the experiment, a hardware model of an active magnetic bearing system is constructed in the laboratory as depicted

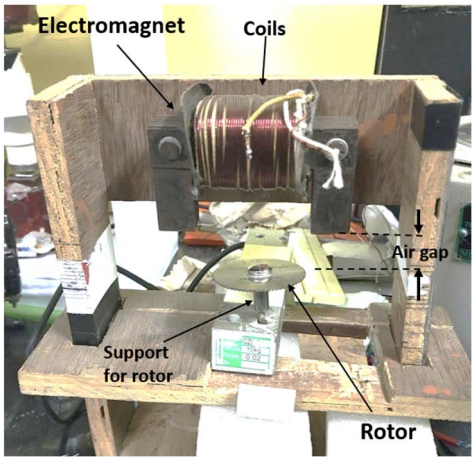


**FIGURE 2.** Fabricated model of the proposed active magnetic bearing system.

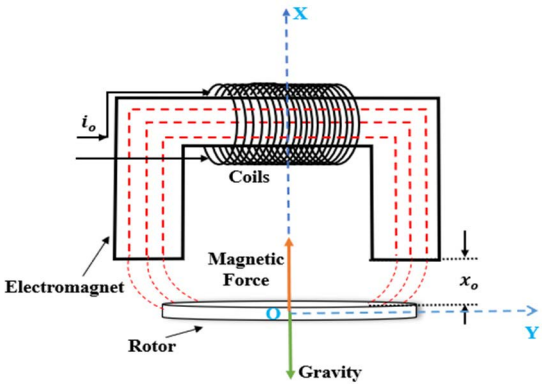


**FIGURE 3.** Simplified diagram of the active magnetic bearing system.

in Figure 2. Here, the electromagnet and rotor (suspending object) are made of iron having a relative permeability of 11000 and 5000 respectively. On the horizontal limb of the electromagnet, the copper winding is stacked which has a relative permeability of 0.88 and thickness of 17 SWG [18]. To calculate resistance and inductance of electromagnet some tests are performed in the laboratory [26] and obtained results are- resistance of the coil ($R$) = 1.2 ohms, inductance of coil ($L_{coil}$) = 20.598 mH. Rotor of this AMB system is of disk shaped having a mass($m$) of 0.0654 Kg.

Some assumptions need to be made before modeling an AMB system. It is assumed that at first electromagnet is not magnetized. The energy given to the coils of the electromagnet is fully utilized and converted into magnetic energy [22]. This generated energy in form of the magnetic field passes through the rotor considering magnetic hysteresis and the leakage flux is negligible due to the very small air gap between electromagnet and rotor [16], [27].

### B. ANALYSIS OF ACTIVE MAGNETIC BEARING SYSTEM

A simplified diagram of the AMB system is shown in Figure 3,

According to Maxwell's electromagnetic theory, Magnetic force ($F_{EM}$)exerted by a single electromagnet is formulated as [28],

$$F_{EM}(i_{coil}, x) = C\frac{i_{coil}^2}{x^2} \tag{1}$$

where, $i_{coil}$ = current in electromagnet coil, $x$ = air gap between electromagnet and rotor, and $C$ = a constant represents as,

$$C = \frac{1}{4}\mu_o N_{coil}^2 A_{EM} \tag{2}$$

here, $\mu_o$ = permeability of vacuum = $1.257 * 10^{-7}$ H/m, $N_{coil}$ = number of coils turn in electromagnet and $A_{EM}$ = cross-sectional area of the pole of the electromagnet.

A small change in the air gap ($\delta x$) between the electromagnet and rotor leads to a change in coil current ($\delta i_{coil}$) of the electromagnet, Equation 1 can represent as,

$$F_{EM}(i_{coil}, x) = C\frac{(i_{coil} + \delta i_{coil})^2}{(x - \delta x)^2} \tag{3}$$

Equation3 is nonlinear and hence Taylor series expansion is used to linearize the system equation at a nominal point of operation i.e., $i_{coil} = i_o$ and $x = x_o$,

$$F_{EM} \approx F_{EM}(i_o, x_o) + \left.\frac{\partial F_{EM}}{\partial x}\right|_{(i_o, x_o)} (x - x_o) + \left.\frac{\partial F_{EM}}{\partial i_{coil}}\right|_{(i_o, x_o)} (i_{coil} - i_o) + \ldots \tag{4}$$

Simplifying Equation 4 and after neglecting the higher-order terms, we can get,

$$F_{EM}(i_o, x_o) = C_a i_o + C_z x_o \tag{5}$$

where, $C_a$ and $C_z$ are constant for the nominal operating point ($i_o, x_o$) and can be calculated as,

$$C_a = \frac{\mu_o A_{EM} N_{coil}^2 i_o}{x_o^2}$$
$$C_Z = \frac{\mu_o A_{EM} N_{coil}^2 i_o^2}{x_o^3} \tag{6}$$

Analyzing further, in Figure 3, at point 'O' during nominal operation the dynamics can be given as,

$$F_{EM}(i_o, x_o) = m\frac{d^2 x_o}{dt^2} \tag{7}$$

Solving the Equation 5 and Equation 7 using Laplace transform and arranging in we can get the transfer function of the proposed AMB system in $s$- domain which is,

$$T_{AMB}(s) = \frac{X(s)}{I(s)} = \frac{C_a}{ms^2 - C_z} \tag{8}$$

For the fabricated model of AMB depicted in Figure 1 nominal operating point ($i_o, x_o$) are taken as –

$$i_o = 2.44A$$
$$x_o = 0.01m$$

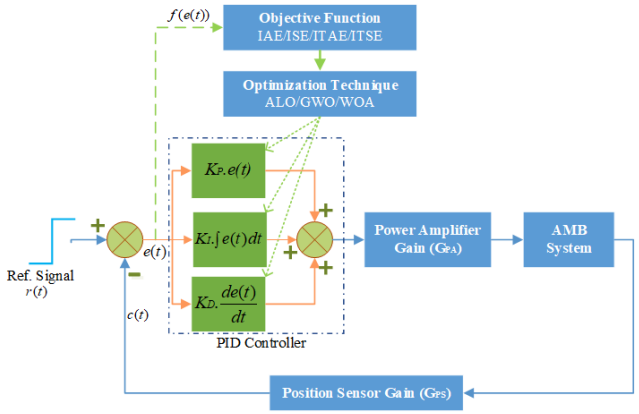


**FIGURE 4.** Proposed closed-loop control of AMB system.

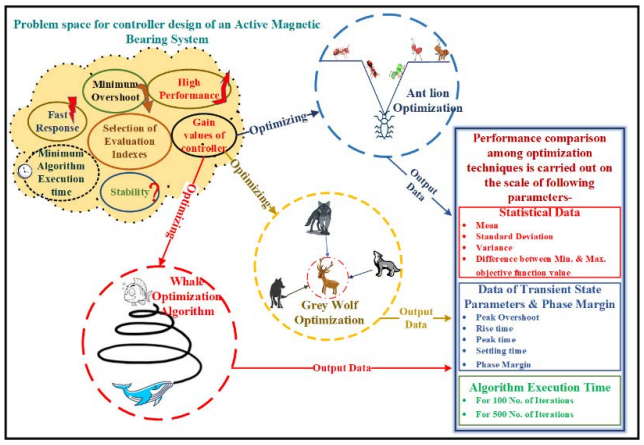


**FIGURE 5.** Complete pictorial representation of the manuscript.

At equilibrium, from Equation 6, $C_a$ and $C_z$ are calculated for the proposed system, using these values a transfer function at a 10 mm air gap (equilibrium position) is calculated as,

$$T_{AMB}(s) = \frac{7.69}{s^2 - 1877.49} \tag{9}$$

The open-loop transfer function of Equation9 has a pole on the right side of the imaginary ($jw$) axis. Therefore, this system is unstable and for proper operation, a closed loop is needed consisting controller and power amplifier as depicted in Figure 4.

The proposed closed-loop AMB system is shown in above Figure 4, where $G_{PA}$ is power amplifier gain and $G_{PS}$ is position sensor gain parameter [29]. Both parameters are constant for a model. The objective function is formed using an error signal and the optimization technique is implemented to minimize the error. Gain parameters of the PID controller are optimized using three different metaheuristic hunting-based algorithms. Those algorithms are further explained in the next section.

Problems associated with the controller design along with the complete work of the manuscript is represented in a pictorial form as shown in Figure 5.

## III. HUNTING-BASED OPTIMIZATION ALGORITHMS

### A. ANT LION OPTIMIZATION (ALO) ALGORITHM

In the field of natural-inspired hunting mechanism-based optimization, Ant Lion Optimization (ALO) is one of the advantageous optimization technique proposed by

S. Mirjalili [30] in 2015. ALO resembles the natural hunting mechanism of grey antlions and their preferred attack target is ants. This algorithm incorporates population-based and local-based search strategies to form a smart algorithm that can perform both, global exploration and local exploitation search [31] for a given optimization problem. The process of hunting ants by ant lions is graphically represented in Figure 6, later this optimization algorithm is explained mathematically and in a flowchart.

The algorithm starts by initialization of population of ants ($A$) and antlions($A_L$) in a dimension ($d$) with a maximum

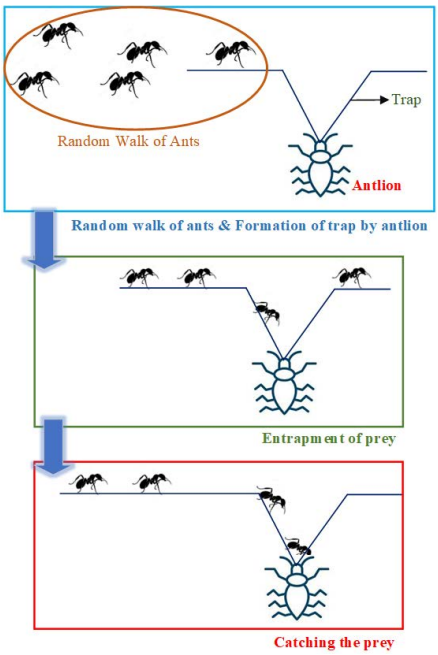


**FIGURE 6.** Graphical presentation of ant lion optimization algorithm.

number of iterations ($T$). As ants travel stochastically in nature when looking for food, a random walk is used to represent their movement as follows [30]:

$$x_i(t) = [0, cumsum(2r(t_1) - 1), cumsum(2r(t_2) - 1), \ldots .cumsum(2r(t_T) - 1)] \tag{10}$$

where, $x_i(t)$ = random walk of $i^{th}$ant, $cumsum$ refers to cumulative summation, $T$ = maximum number of iterations, $t_1$ shows the $1^{st}$ iteration and $r(t)$ is a random function that is given by,

$$r(t) = \begin{cases} 1 & if\ rand > 0.5 \\ 0 & if\ rand \leq 0.5 \end{cases} \tag{11}$$

where $rand$ is a randomly generated number in the interval [0, 1] and $t$ = iteration index

As it is a population-based algorithm, so the position of each ant and antlion is stored in a matrix form where the number of columns is the dimension($d$), as shown in Equation 12.

$$P_{Ant} = \begin{bmatrix} A_{1,1} & \cdots & A_{1,d} \\ \vdots & \ddots & \vdots \\ A_{n,1} & \cdots & A_{n,d} \end{bmatrix}$$
$$P_{Antlion} = \begin{bmatrix} A_{L_{1,1}} & \cdots & A_{L_{1,d}} \\ \vdots & \ddots & \vdots \\ A_{L_{n,1}} & \cdots & A_{L_{n,d}} \end{bmatrix} \quad (12)$$

where, $P_{Ant}$ = stores position of ants, $P_{Antlions}$ = stores position of antlions, $A_{k,m}$ or, $A_{Lk,m}$ shows the $k^{th}$ ant or, antlion position at $m^{th}$ dimension, $n$ = number of ants, and $d$ = number of dimensions

Using the objective function, ants and antlions are evaluated and results are stored in a matrix as shown in Equation 13,

$$P_{OAnt} = \begin{bmatrix} f([A_{1,1}, A_{1,2} \ldots., A_{1,d}]) \\ \vdots \\ f([A_{n,1}, A_{n,2} \ldots., A_{n,d}]) \end{bmatrix}$$
$$P_{OAntlion} = \begin{bmatrix} f([A_{L_{1,1}}, A_{L_{1,2}} \ldots., A_{L_{1,d}}]) \\ \vdots \\ f([A_{L_{n,1}}, A_{L_{n,2}} \ldots., A_{L_{n,d}}]) \end{bmatrix} \quad (13)$$

where, $P_{OAnt}$ = stores fitness value of ants, $P_{OAntlions}$ = stores fitness value of antlions, $A_{k,m}$ or, $A_{Lk,m}$ shows the $k^{th}$ ant or, antlion value at $m^{th}$ dimension, $n$ = number of ants, $d$ = number of dimensions, and $f$ = objective function.

To maintain ants walking randomly inside the search region, Equation 14 is used to update the position of each ant [30],

$$X_i(t) = \frac{(X_i^t - a_i)(D_i^t - C_i^t)}{b_i - a_i} + C_i^t \quad (14)$$

where, $a_i$ = minimum value of random walk of $i^{th}$ variable, $b_i$ = maximum value of random walk of $i^{th}$ variable, $C_i^t$ and $D_i^t$ shows the minimum and maximum value of the $i^{th}$ variable at $t^{th}$ iteration respectively.

Antlion traps have an effect on the random walk of ants Equation 15 and Equation 16 are given to mathematically describe this assumption,

$$C_i^t = A_{L_k}^t + C^t; D_i^t = A_{L_k}^t + D^t \quad (15)$$
$$C^t = \frac{C^t}{I}; D^t = \frac{D^t}{I} \quad (16)$$

here, $C^t$ and $D^t$ is the minimum and maximum value of all variables at iteration $t$ respectively, similarly, $C_i^t$ and $D_i^t$ is the minimum and maximum of all variables for $i^{th}$ ant at iteration $t$ respectively, $A_{L_k}^t$ represents position of $k^{th}$ antlion at iteration $t$ and $I$ is a sliding ratio represented by Equation 17,

$$I = 10^v \frac{t}{T} \quad (17)$$

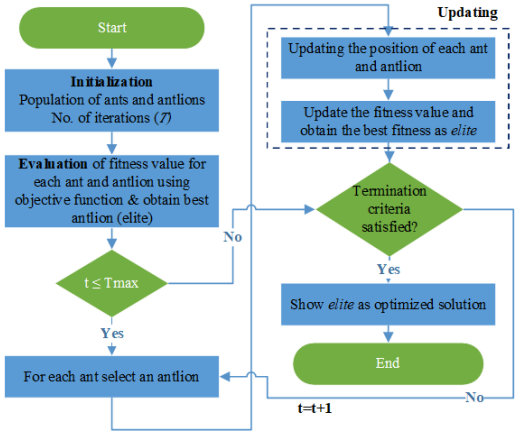


**FIGURE 7.** Flowchart of ant lion optimization (ALO) algorithm.

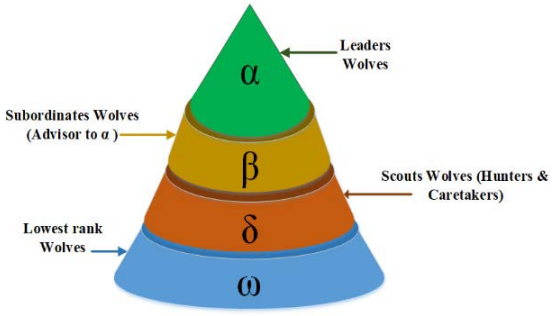


**FIGURE 8.** The hierarchical order of grey wolf society.

where, $t$ = current iteration, $T$ = maximum iteration, and $v$ changes as Equation 18,

$$v = \begin{cases} 2, & if\ t > 0.1T \\ 3, & if\ t > 0.5T \\ 4, & if\ t > 0.75T \\ 5, & if\ t > 0.9T \\ 6, & if\ t > 0..95T \end{cases} \quad (18)$$

All ant motions are influenced by the fittest antlion and this finest antlion is designated an elite. As a result, it is believed that every ant goes around a randomly picked antlion by the roulette wheel and the elite at the same time as follows [32],

$$A_i^t = \frac{R_A^t + R_E^t}{2} \quad (19)$$

here, $R_A^t$ is the roulette wheel-selected random walk around the antlion at iteration $t$, $R_E^t$ is random walk around elite at iteration $t$ and $A_i^t$ represents the position of $i^{th}$ ant at iteration $t$.

To simulate the final step of hunting, when the ant is drawn into the sand and eaten. Then, antlion updates its position following the Equation 20,

$$A_{L_i}^t = A_i^t if A_i^t < A_{L_i}^t \quad (20)$$

A generalized flowchart for this algorithm is depicted in Figure 7.

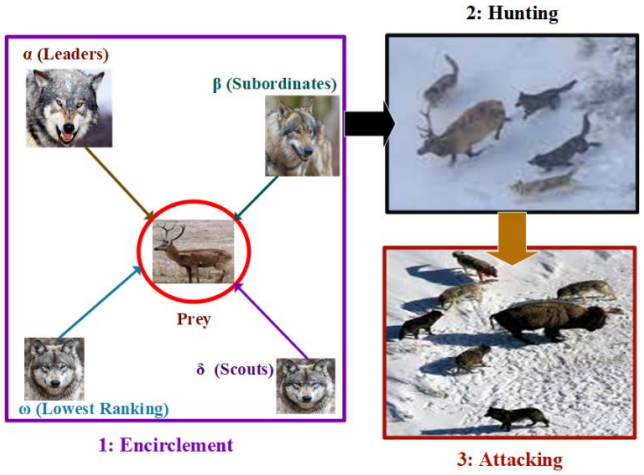


**FIGURE 9.** Pictorial representation of grey wolf optimization algorithm.

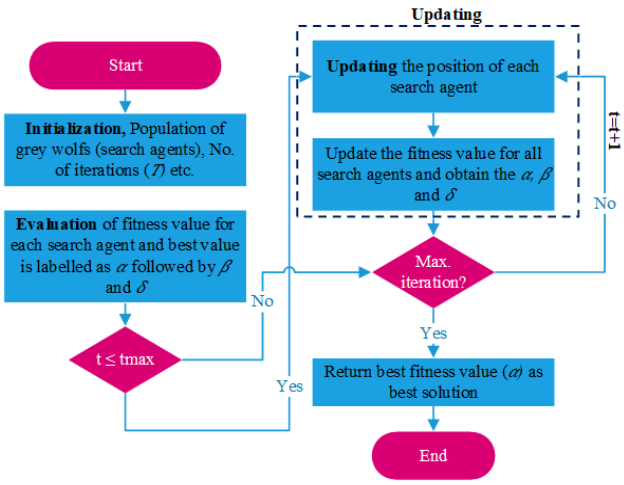


**FIGURE 10.** Flowchart of grey wolf optimization (GWO) algorithm.

The ALO algorithm efficiently handles applications from a wide range of fields including engineering [33] computer science, mathematics, medicine, energy, etc [31].

### B. GREY WOLF OPTIMIZATION (GWO) ALGORITHM

Another famous optimization technique based on the hunting mechanism of wolves is Grey wolf optimization (GWO), proposed by S. Mirjalili et. al., in 2014 [34]. It imitates the process of surrounding, encircling, and attacking the prey by a grey wolf pack. Wolves establish cooperative groupings known as packs to live in the hazardous and competitive outdoor environment.

Depending upon their fitness value, from top to bottom, the grey wolf society is organized in rigid hierarchical order as depicted in Figure 8 [35]. The topmost order is the leader wolf, alpha ($\alpha$), having the best fitness value. The leaders of a pack of grey wolves (alpha) are frequently in charge of making decisions for their pack such as where to sleep, where to hunt, and when to get up. Most of the time, the rest of the pack must obey the alpha's choice. The second topmost order in the hierarchical society of grey wolves is the beta ($\beta$) wolf and the beta's function is to assist the alpha in making judgments. Beta can be either male or female wolves, and beta is the ideal candidate for alpha replacement. The order next to beta is the delta ($\delta$), the delta wolves obey the $\alpha$and $\beta$ wolves and rule the omega ($\omega$) wolves. In the pack, they serve as caretakers, hunters, scouts and elders. The lowest order in the hierarchy of grey wolves is omega ($\omega$), which serves as a scapegoat. The wolves at the $\omega$ level must accept other wolves' directives and are the last wolves to be permitted to devour food [36]. At first, the number of grey wolves (search agents) and a number of iterations are initialized and using them grey wolf optimization (GWO) algorithm can be mathematically modeled in the following three steps [37] a pictorial representation of which is depicted in Figure 9.

#### 1) ENCIRCLEMENT

During the hunt, the very initial stage is to track and encircle the prey. Equation 21 and Equation 22 are used to mathematically describe the encircling behavior.

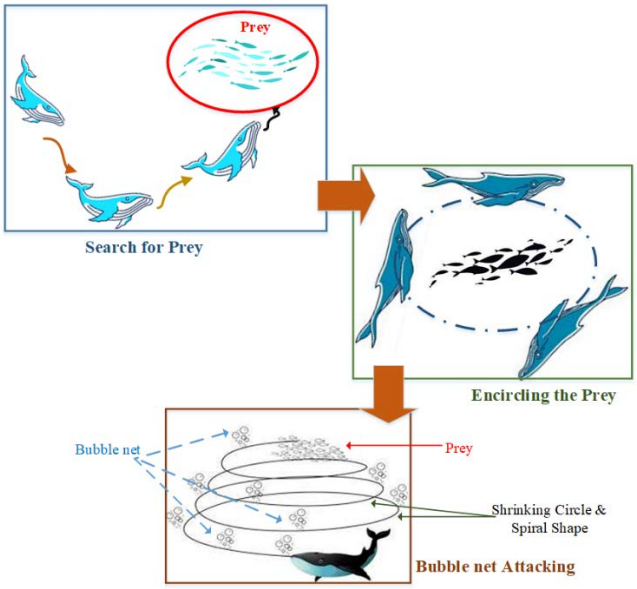


**FIGURE 11.** Hunting process of humpback whales in WOA.

$$X_{t+1} = X_{P_t} - A.D \tag{21}$$

$$D = \left|C.X_{P_t} - X_t\right| \tag{22}$$

where, $X_t$ = position of the grey wolf at $t^{th}$ iteration, $X_{t+1}$ = position of the grey wolf at $(t+1)^{th}$ position, $X_{P_t}$ = prey's position, $A$, and $C$ are coefficient vectors that can be represented as,

$$A = 2r_1.a - a$$
$$C = 2r_2 \tag{23}$$

where, $r_1$ and $r_2$ are random vector in [0, 1], components of $a$ are linearly decreased from 2 to 0 with increment in iterations with the help of Equation 24,

$$a = 2.\left(1 - \frac{t}{t_{max}}\right) \tag{24}$$

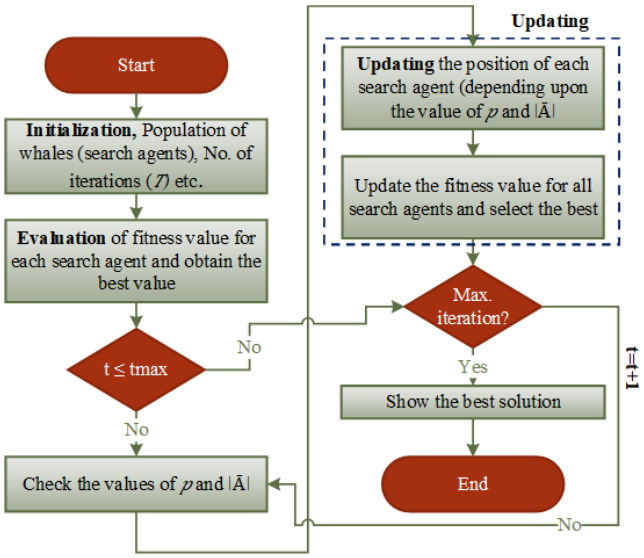


**FIGURE 12.** Flowchart of whale optimization algorithm (WOA).

here, $t$ = current iteration and $t_{max}$ = maximum number of iterations

With the help of Equation 21 and Equation 22, the grey wolf updated its location around the prey.

### 2) HUNTING

Grey wolf pack hunt together and the hunting is commanded by the alpha. The alpha may choose which possible prey to follow, or he may opt to abandon the hunt if things aren't going well. The beta and delta may occasionally join in the hunting. It is supposed that $\alpha$, $\beta$, and $\delta$ have the most hunting experience and they can predict the most possible position of prey. The omegas follow the lead of $\alpha$, $\beta$, and $\delta$. As a result, this collective hunting behavior is mathematically represented as,

$$\begin{aligned} D_{\alpha} &= \left|C_1 X_{\alpha_t} - X_t\right| \\ D_{\beta} &= \left|C_2 X_{\beta_t} - X_t\right| \\ D_{\delta} &= \left|C_3 X_{\delta_t} - X_t\right| \\ X_1 &= X_{\alpha_t} - A_1 D_{\alpha} \\ X_2 &= X_{\beta_t} - A_2 D_{\beta} \\ X_3 &= X_{\delta_t} - A_3 D_{\delta} \\ X_{t+1} &= \frac{X_1 + X_2 + X_3}{3} \end{aligned} \tag{25}$$

where, $X_{\alpha_t}$, $X_{\beta_t}$, $X_{\delta_t}$ and $X_t$ represents the position of $\alpha$, $\beta$, $\delta$, and $\omega$ wolves respectively at $t^{th}$ iterations.

### 3) ATTACKING

The grey wolves encircled the prey when it stops moving and conclude the hunt by attacking the prey. To mathematically represent approaching the prey, the value of $a$ is reduced linearly from 2 to 0 in Equation 23 and due to this the value of $A$ gets changed in the range $[-2a, 2a]$. So, it may represent as follow,

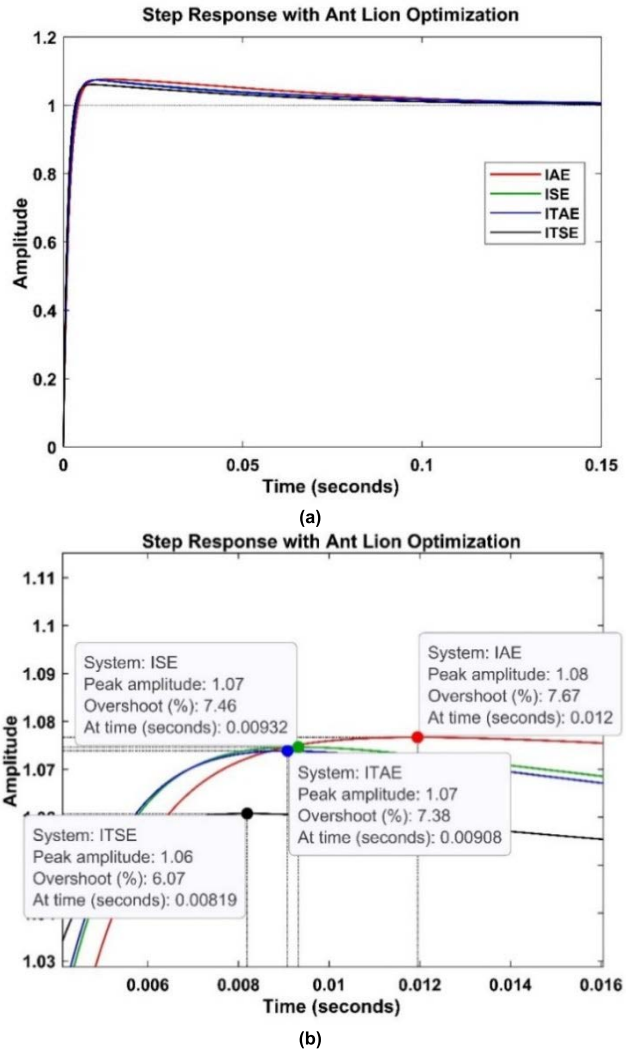


**FIGURE 13.** (a) Step response of proposed closed-loop AMB system observed by implementing ALO with IAE, ISE, ITAE, and ITSE objective functions, (b) for time, 0.005sec- 0.016 sec.

If $|A| \geq 1$,exploration means it compels the grey wolves to deviate from the current prey in the hope of finding a fitter prey.

If $|A| < 1$, exploitation means the grey wolves attack the prey and finish it.

A flow chart for the implementation of the GWO algorithm is shown in Figure 10.

Application of GWO algorithm is in various fields like engineering, control, power system, electromagnetics, etc [37], [38].

## C. WHALE OPTIMIZATION ALGORITHM (WOA)

In 2016, S. Mirjalili and A. Lewis have proposed a novel optimization technique named Whale Optimization Algorithm [39] to metaheuristic algorithms. Whales are thought to be extremely intelligent creatures, as they have double the amount of spindle cells as an adult human [40]. It has been found that whales can think, learn, assess, communicate, and even get emotional in the same way that humans do,

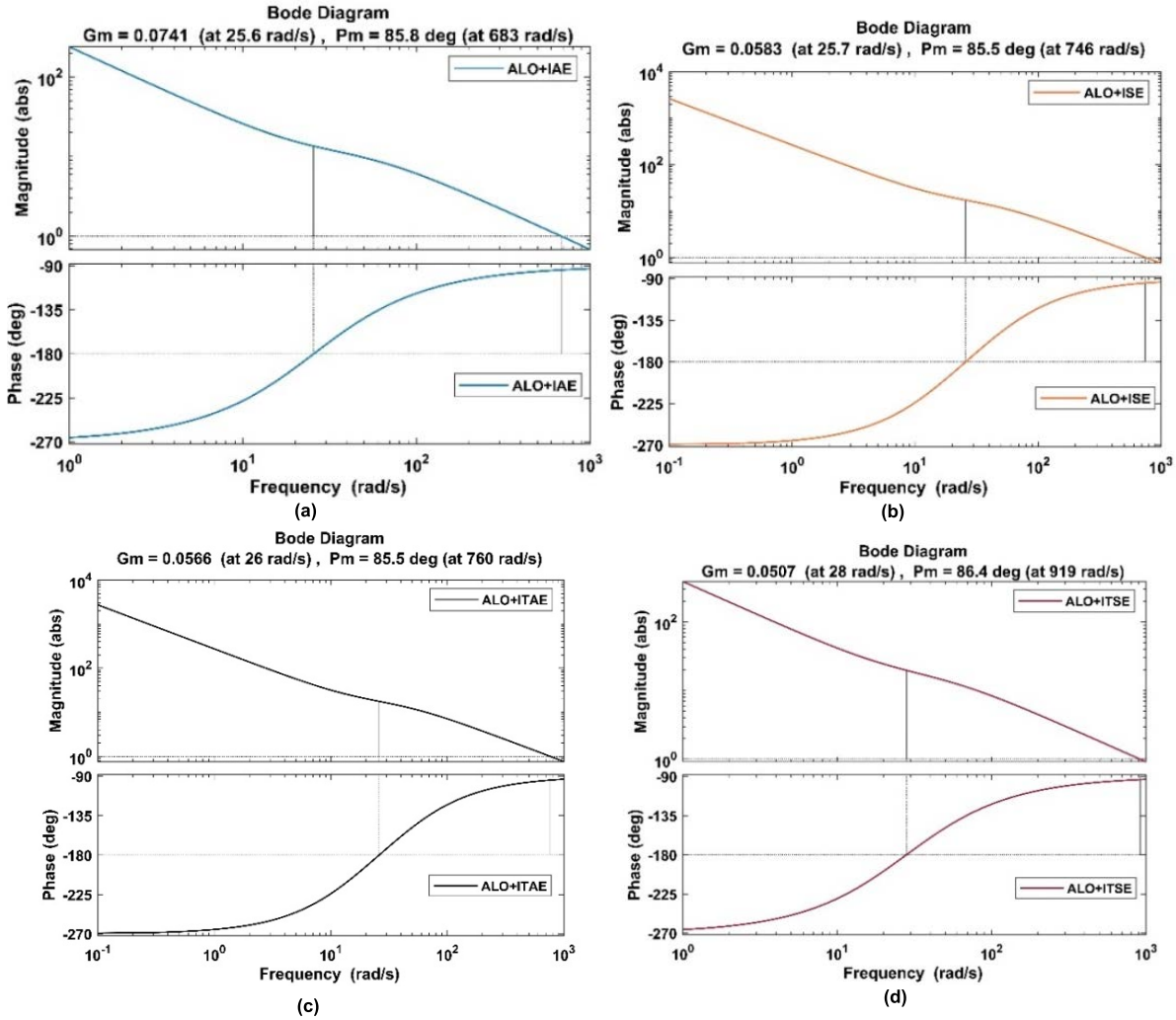


**FIGURE 14.** Bode plot of proposed closed-loop AMB system optimized by ALO with (a) IAE (b) ISE (c) ITAE and (d) ITSE objective functions.

but at a far lower level of intelligence. Whales (particularly killer whales like humpback whales) have been discovered to be capable of developing their own vernacular. These killer whales are a little slow and because of that, they are not able to chase and swallow their prey, due to this they hunt in a very special manner. Their hunting activity is referred to as the bubble-net feeding approach which is a unique activity found solely in humpback whales[41]. An image describing the whale hunting process is illustrated in Figure 11.

This algorithm begins with the initialization of whale population in $n$ dimensional search space for $T$ number of iterations and the WOA is a mathematical model in the following parts [42]-

### 1) ENCIRCLING THE PREY

In this algorithm, it is considered that the current best solution is the finest one and all the other search agents strive to improve their positions to become the finest search agent. That can be mathematically represented as Equation 26,

$$\vec{X}(t+1) = \vec{X}^*(t) - \vec{A}.\left|\vec{C}.\vec{X}^*(t) - \vec{X}(t)\right| \tag{26}$$

where,

$$\vec{D} = \left|\vec{C}.\vec{X}^*(t) - \vec{X}(t)\right| \tag{27}$$

here, $t$ = current iteration, $\vec{X}^*$ = position vector of the best solution, $\vec{X}$ = position vector, $\vec{A}$ and $\vec{C}$ are linear coefficient vectors that can be defined as Equation 28,

$$\begin{aligned} \vec{A} &= 2\vec{a}.\vec{r} - \vec{a} \\ \vec{C} &= 2.\vec{r} \end{aligned} \tag{28}$$

where, $\vec{r}$ = random vector in the range [0,1] and $\vec{a}$ = a vector that linearly decreased from 2 to 0 with an increment in iteration number.

### 2) BUBBLE NET ATTACKING

After encircling the humpback whales swim around the fish school in a shrinking circle and along a spiral-shaped path simultaneously. It is assumed that there is a 50% chance of selecting either the shrinking encircling method or the

**TABLE 1. Parameters required for initialization of ALO algorithm.**

| S No. | Parameters | Representation | Value |
|---|---|---|---|
| **1.** | Number of Ants | $A$ | 50 |
| **2.** | Number of Antlions | $A_L$ | 50 |
| **3.** | No. of iterations | $T$ | 100 |
| **4.** | Lower bound | $lb$ | [0,0,0] |
| **5.** | Upper bound | $ub$ | [10,100,0.15] |

**TABLE 2. Optimized PID controller values for proposed AMB system using ALO.**

| Sl. No | Optimization method | Objective function | $K_P$ | $K_I$ | $K_D$ | $\frac{s^2K_D + sK_p + K_I}{s}$ |
|---|---|---|---|---|---|---|
| 1. | Ant lion optimization (ALO) | IAE | 4.446 | 58.235 | 0.089 | $\frac{0.089s^2 + 4.446s + 58.235}{s}$ |
| | | ISE | 5.660 | 64.242 | 0.0971 | $\frac{0.09710s^2 + 5.6609s + 64.24}{s}$ |
| | | ITAE | 5.862 | 66.736 | 0.099 | $\frac{0.099s^2 + 5.8620s + 66.736}{s}$ |
| | | ITSE | 6.828 | 94.101 | 0.1196 | $\frac{0.11961s^2 + 6.8281s + 94.10}{s}$ |

spiral model to update the position of whales throughout the optimization. mathematically it can be shown as,

$$\vec{X}(t+1) = \begin{cases} \vec{X}^*(t) - \vec{A}.\vec{D} & if\ p < 0.5 \\ \vec{D}'.e^{bl}.\cos(2\pi l) + \vec{X}^*(t) & if\ p \geq 0.5 \end{cases} \tag{29}$$

where $p$ is a random number in the range [0,1]

### 3) SEARCH FOR PREY

De facto the humpback whales randomly search for prey. Therefore, to improve the optimization and to perform a global search, the position of a search agent in this exploration phase is determined by a randomly picked search agent rather than the best search agent discovered thus far. This method along with $\vec{A} > 1$ can be mathematically modeled as,

$$\vec{X}(t+1) = \vec{X}_{rand}(t) - \vec{A}.\left|\vec{C}.\vec{X}_{rand}(t) - \vec{X}(t)\right|$$
$$\vec{X}(t+1) = \vec{X}_{rand}(t) - \vec{A}.\vec{D} \tag{30}$$

here, $\vec{X}_{rand}$ = randomly chosen position vector from the current population

A flowchart for WOA is shown in Figure 12.

The whale optimization algorithm is frequently utilized in a variety of fields like aerospace, management, robotics, cloud computing, energy, etc [41], [43].

## IV. RESULTS AND DISCUSSION

This section of the manuscript presents three different nature-inspired hunting-based optimization techniques to control the proposed closed-loop active magnetic bearing system. These three optimization methods are- Ant lion optimization, grey wolf optimization, and whale optimization algorithm.

**TABLE 3. Obtained value of transient state parameters, final value of objection function, and phase margin using ALO.**

| Sl. No. | Optimization method | Objective function | $\%M_p$ | $t_r$ (sec) | $t_p$ (sec) | $t_s$ (sec) | $E_{ss}$ | $J$ | $P.M$ (in degree) |
|---|---|---|---|---|---|---|---|---|---|
| 1. | Ant lion optimization (ALO) | IAE | 7.67 | 0.00268 | 0.01190 | 0.09094 | 0.001 | 1.00 90 | 85.8 |
| | | ISE | 7.46 | 0.00244 | 0.00932 | 0.09004 | 0.001 | 1.00 80 | 85.5 |
| | | ITAE | 7.38 | 0.00239 | 0.00908 | 0.08075 | 0.001 | 0.50 45 | 85.5 |
| | | ITSE | 6.07 | 0.00204 | 0.00819 | 0.07111 | 0.001 | 0.50 40 | 86.4 |

These algorithms are used to tune the PID controller of the proposed closed system in such a way that the proposed system becomes stable for the nominal operating position. Gains values obtained by these optimization methods are calibrated based on four well-established integral performance indices which are listed as follows [44] -

1. Integral of absolute error (IAE),

$$IAE = \int_0^T |e(t)|\,dt \tag{31}$$

2. Integral of squared error (ISE),

$$ISE = \int_0^T e^2(t)\,dt \tag{32}$$

3. Integral of time multiplied absolute error (ITAE)

$$ITAE = \int_0^T t\,|e(t)|\,dt \tag{33}$$

4. Integral of time multiplied squared error (ITSE),

$$ITSE = \int_0^T t.\left(e^2(t)\right)dt \tag{34}$$

where, $e(t)$ = error signal which can be calculated as,

$$e(t) = r(t) - c(t) \tag{35}$$

where, $r(t)$ = reference signal and $c(t)$ = feedback signal

The above-listed four performance indices are used as the objective function in the optimization process to minimize error signal magnitude. The optimization methods are hunting-based algorithms and the first one is ALO.

### A. IMPLEMENTATION OF ANT LION OPTIMIZATION (ALO) ALGORITHM

In the initialization process of ALO value of some parameters need to be defined, those parameters with their assumed values for optimization are listed in Table 1.

As PID controllers have three variable gain parameters (i.e., proportional gain ($K_P$), integral gain ($K_I$) and derivative gain ($K_D$)) so, the number of dimensions is considered three

**TABLE 4. Parameters required for initialization of GWO algorithm.**

| S No. | Parameters | Representation | Value |
|---|---|---|---|
| 1. | Number of grey wolves | $N$ | 50 |
| 2. | No. of iterations | $T$ | 100 |
| 3. | Lower bound | $lb$ | [0,0,0] |
| 4. | Upper bound | $ub$ | [10,100,0.15] |

for implementing the ALO algorithm. For each objective function, execution of the ant lion algorithm is carried out as depicted in flow chart Figure 7 for $T$ number of iterations. After termination criteria, the algorithm gives the optimized value of gain parameters of the PID controller which are listed in Table 2.

The performance of the controller with the obtained optimized gain values in a closed loop with the proposed system needs to be studied. For this purpose, a unit step signal for 0.15 seconds is applied to the proposed closed-loop system and a step response is observed as shown in Figure 13.

This step response analysis has complete data of transient state performance of the closed-loop system with an optimized controller as are listed in Table 3 here, $\%M_p$ represents peak overshoot, $t_r$ represents rise time in seconds, $t_p$ is peak time in seconds, $t_s$ is settling time in seconds, $E_{ss}$ is a steady-state error and $J$ is the final value of the objective function.

Observed time-domain analysis represents that with ITSE objective function peak overshoot got reduced as compared to IAE, ISE, and ITAE objective function. In addition to this rise time, peak time, and settling time get reduced too which leads to faster system response.

To understand the system stability, the bode diagram is plotted as shown in Figure 14. Here it is observable that the maximum phase margin (P.M) is allowed by the ITSE objective function having a value of $86.4^0$ at an absolute gain margin of 0.0507.

Ant lion optimization based on IAE, ISE, and ITAE objective functions shows almost the same transient state characteristics. But ALO-ITSE performance dominates in every aspect rather it is time-domain analysis or, stability analysis.

### *B. IMPLEMENTATION OF GREY WOLF OPTIMIZATION (GWO) ALGORITHM*

Some parameters must be defined to implement the GWO algorithm. Table 4 contains the list of those variables.

Here, the lower and upper bound are the minimum and maximum allowable limits for the gain value of the PID controller. Which means the range of proportional gain ($K_p$) is limited to [0, 10], integral gain ($K_I$) is limited to [0, 100] and derivative gain ($K_D$) is limited to [0, 0.15] respectively. Using Equation 21-Equation 25 and following the flowchart shown in Figure 10 this GWO algorithm is executed for $T$ no. of iterations and the realized gain values of the PID controller are presented in Table 5.

To illustrate the effectiveness of GWO optimized PID controller for the proposed closed-loop system a step response analysis is carried out by applying a unit step signal for

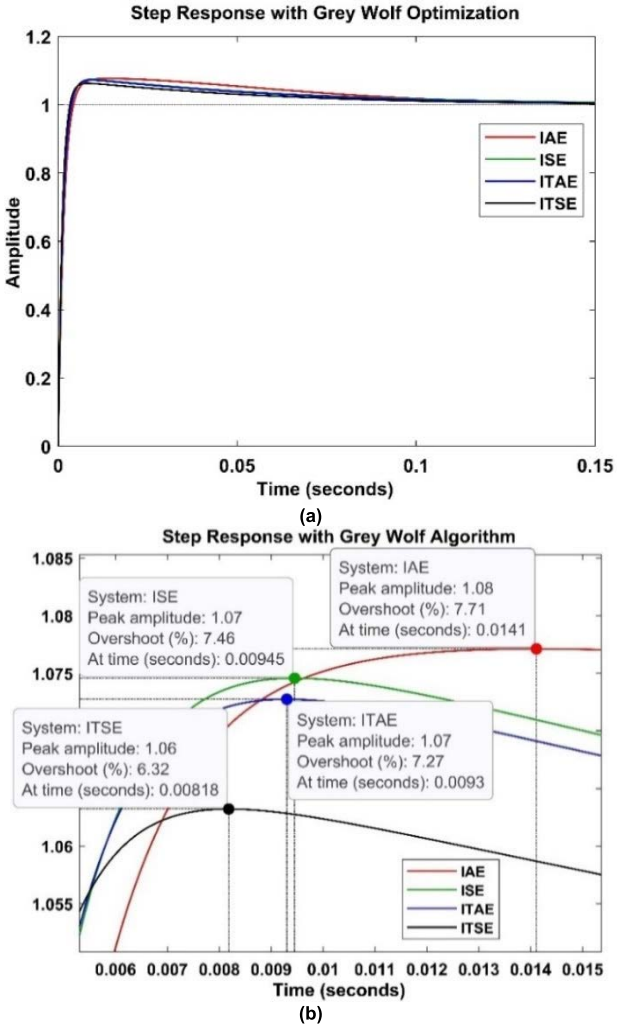


**FIGURE 15. (a) Step response of proposed closed-loop AMB system observed by implementing GWO with IAE, ISE, ITAE, and ITSE objective functions, (b) for time, 0.006 sec - 0.015 sec.**

**TABLE 5. Optimized PID controller values for proposed AMB system using GWO method.**

| Sl. No | Optimization method | Objective function | $K_p$ | $K_I$ | $K_D$ | $\frac{s^2K_D + sK_p + K_I}{s}$ |
|---|---|---|---|---|---|---|
| 1. | Grey Wolf Optimization | IAE | 4.1032 | 60.712 | 0.08756 | $\frac{0.08756s^2 + 4.1032s + 60.71}{s}$ |
| | | ISE | 5.5652 | 63.509 | 0.09660 | $\frac{0.0966s^2 + 5.5652s + 63.509}{s}$ |
| | | ITAE | 5.7203 | 70.454 | 0.09944 | $\frac{0.09944s^2 + 5.7203s + 70.45}{s}$ |
| | | ITSE | 6.7895 | 88.407 | 0.11606 | $\frac{0.11606s^2 + 6.7895s + 88.40}{s}$ |

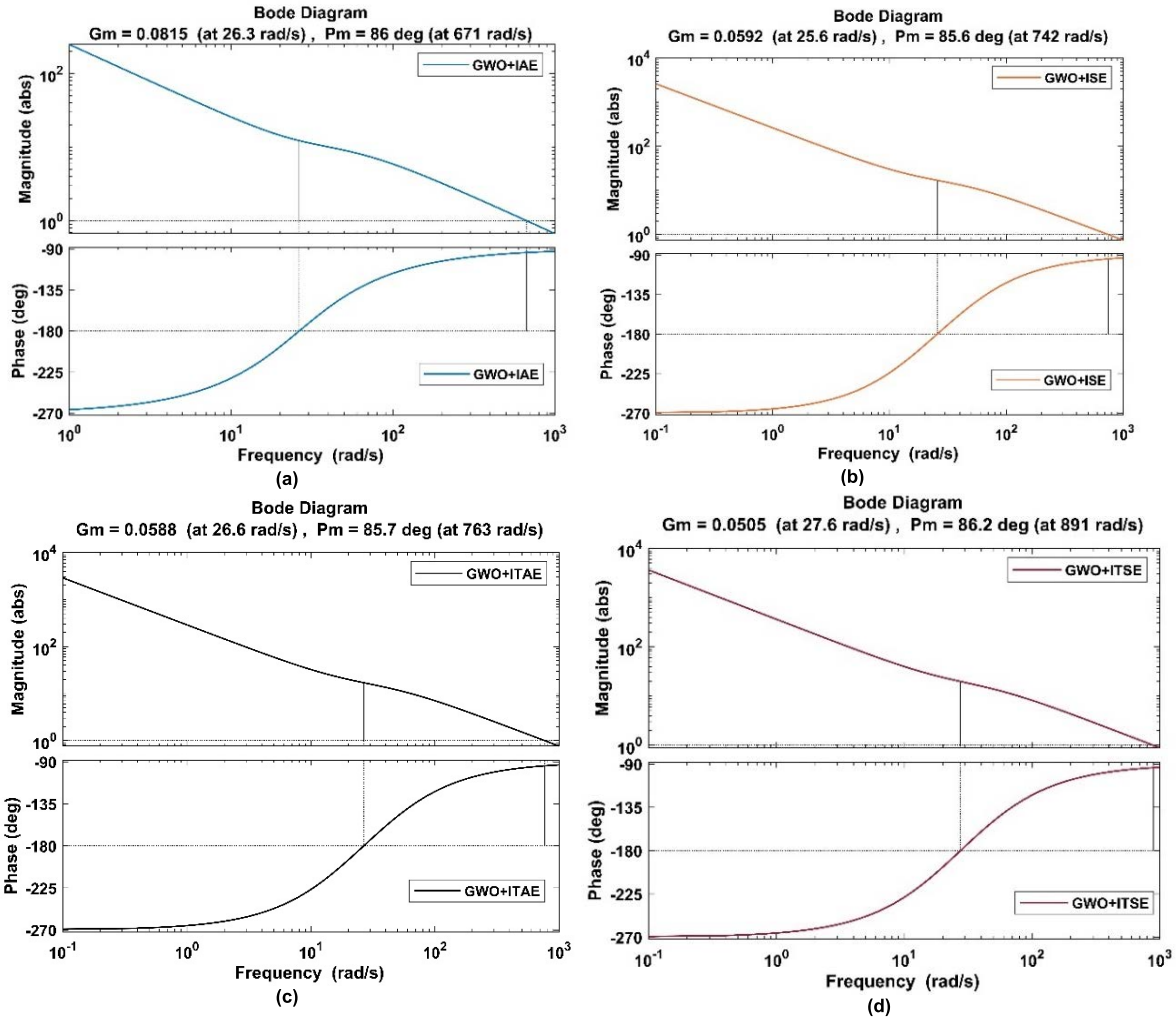


**FIGURE 16.** Bode plot of proposed closed-loop AMB system optimized by GWO with (a) IAE (b) ISE (c) ITAE and (d) ITSE objective functions.

**TABLE 6.** Obtained value of transient state parameters, final value of objection function, and phase margin using GWO.

| Sl. No. | Optimization method | Objective function | $\%M_p$ | $t_r$ (sec) | $t_p$ (sec) | $t_s$ (sec) | $E_{ss}$ | $J$ | $P.M$ (in degree) |
|---|---|---|---|---|---|---|---|---|---|
| 1. | Grey Wolf Optimization (GWO) | IAE | 7.71 | 0.002 74 | 0.014 10 | 0.09 71 | 0.0 01 | 1.00 90 | 86 |
| | | ISE | 7.46 | 0.002 45 | 0.009 45 | 0.09 15 | 0.0 01 | 1.00 80 | 85.6 |
| | | ITAE | 7.27 | 0.002 39 | 0.009 30 | 0.08 53 | 0.0 01 | 0.50 45 | 85.7 |
| | | ITSE | 6.32 | 0.002 09 | 0.008 18 | 0.07 29 | 0.0 01 | 0.50 40 | 86.2 |

0.15 seconds. Step responses of the GWO algorithm with different objective function is depicted in Figure 15.

Parameters of time-domain analysis observed from this step response are shown in Table 6.

From Table 6, it is evident that minimum overshoot ($\%M_p = 6.32$) is attained by ITSE objective function and at the time the speed of the proposed closed-loop is the fastest with a rise time ($t_r$) of 0.00209 sec and settling time ($t_s$) of 0.0729 sec which is minimum as compared to the performance of IAE, ISE, and ITAE objective functions. To study the stability of the proposed system, a bode plot is drawn and the phase margin is observed too as shown in Figure 16.

The Maximum attained phase margin is shown with the ITSE objective function followed by IAE with a value of $86.2^0$ and $86^0$ respectively. ISE and ITAE objective functions have the almost same value of phase margin.

### C. IMPLEMENTATION OF WHALE OPTIMIZATION ALGORITHM (WOA)

Similar to GWO and ALO, to implement a whale optimization algorithm initialization of some parameters is required. Those parameters with their assumed values are listed in Table 7. For a better comparative analysis, the number of whales in WOA, number of antlions in ALO, and number of grey wolves in GWO have the same value. All optimization

**TABLE 7. Parameters required for initialization of WOA method.**

| S No. | Parameters | Representation | Value |
|---|---|---|---|
| 1. | Number of whales | $N$ | 50 |
| 2. | No. of iterations | $T$ | 100 |
| 3. | Lower bound | $lb$ | [0,0,0] |
| 4. | Upper bound | $ub$ | [10,100,0.15] |

**TABLE 8. Optimized PID controller values for proposed AMB system using WOA.**

| Sl. No | Optimization method | Objective function | $K_p$ | $K_I$ | $K_D$ | $\frac{s^2K_D + sK_p + K_I}{s}$ |
|---|---|---|---|---|---|---|
| 1. | Whale Optimization Algorithm (WOA) | IAE | 4.3081 | 58.1265 | 0.0883 | $\frac{0.0883s^2 + 4.3081s + 58.1265}{s}$ |
| | | ISE | 5.3096 | 61.0769 | 0.0953 | $\frac{0.0953s^2 + 5.3096s + 61.0769}{s}$ |
| | | ITAE | 5.8031 | 68.6133 | 0.0997 | $\frac{0.0997s^2 + 5.8031s + 68.6133}{s}$ |
| | | ITSE | 6.7105 | 90.7793 | 0.1143 | $\frac{0.1143s^2 + 6.7105s + 90.7793}{s}$ |

**TABLE 9. Obtained value of transient state parameters, final value of objection function, and phase margin using WOA.**

| Sl. No. | Optimization method | Objective function | $\%M_p$ | $t_r$ (sec) | $t_p$ (sec) | $t_s$ (sec) | $E_{ss}$ | $J$ | $P.M$ (in degree) |
|---|---|---|---|---|---|---|---|---|---|
| 1. | Whale Optimization Algorithm | IAE | 7.68 | 0.00271 | 0.00960 | 0.0997 | 0.001 | 1.0090 | 85.9 |
| | | ISE | 7.44 | 0.00249 | 0.00984 | 0.0997 | 0.001 | 1.0080 | 85.6 |
| | | ITAE | 7.27 | 0.00238 | 0.00917 | 0.0865 | 0.001 | 0.5045 | 85.7 |
| | | ITSE | 6.44 | 0.00212 | 0.00827 | 0.0718 | 0.001 | 0.5040 | 86.2 |

techniques implemented in this paper have the same number of iterations.

To demonstrate the efficacy of these hunting-based algorithms the upper and lower bound of the PID controller are kept the same for all methods. Execution of whale optimization algorithm is carried out in three-dimensional search space for $T$ number of iterations and the obtained value of PID controllers for different objective functions is listed in Table 8.

The effect of these WOA optimized PID controllers on the proposed closed-loop system is studied by applying a step signal for a duration of 0.15sec and the step response is depicted in Figure 17.

With the help of step response values of the various transient state, parameters are observed for different objective functions which are listed in Table 9.

Similar to the observation made in Table 3 of ALO and Table 6 of GWO, In Table 9, the ITSE objective function shows a minimum overshoot $(\%M_p)$ of 6.44 with the least value of rising time $(t_r)$ and settling time $(t_s)$ of 0.00212 sec and 0.0718 sec respectively. From the perspective of stability, the bode plot is shown in Figure 18 and the observed allowable phase margin is $86.2^0$ which is maximum with ITSE objective function at an absolute value of gain margin of 0.0518.

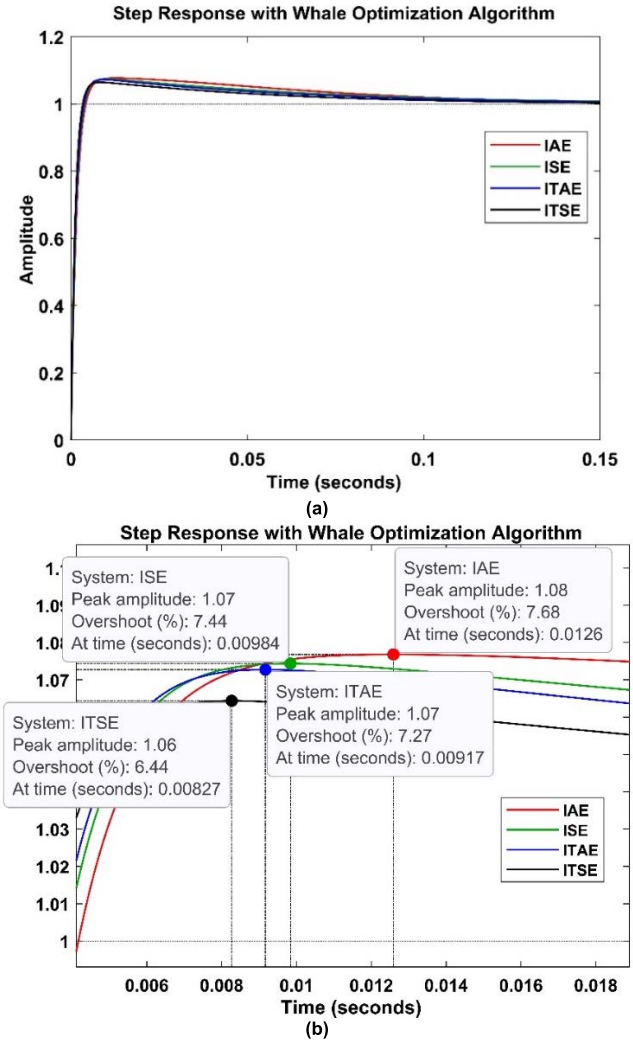


**FIGURE 17. (a) Step response of proposed closed-loop AMB system observed by implementing WOA with IAE, ISE, ITAE, and ITSE objective functions, (b) for time, 0.006 sec - 0.018 sec.**

**TABLE 10. Data of statistical analysis on ant lion optimization (ALO) algorithm.**

| Sl. No. | Parameters | ALO-IAE | ALO -ISE | ALO -ITAE | ALO -ITSE |
|---|---|---|---|---|---|
| 1. | Mean | 1.00899335 | 1.00799241 | 0.50449326 | 0.50398941 |
| 2. | Standard Deviation | 7.7609933e-07 | 1.29151134e-06 | 5.61404299e-07 | 7.32455473e-07 |
| 3. | Variance | 6.02330175e-13 | 1.66800155e-13 | 3.15174787e-13 | 5.36491021e-13 |
| 4. | Minimum value of objective function | 1.00899037 | 1.00798203 | 0.50449279 | 0.50398609 |
| 5. | Maximum value of objective function | 1.00899478 | 1.00798438 | 0.50449323 | 0.50398620 |
| 6. | Difference | 4.5837731e-06 | 2.34695757e-06 | 4.43285096e-07 | 1.18700647e-07 |

With these three optimization techniques, the ITSE objective function shows a better performance in the context of time domain and frequency domain analysis.

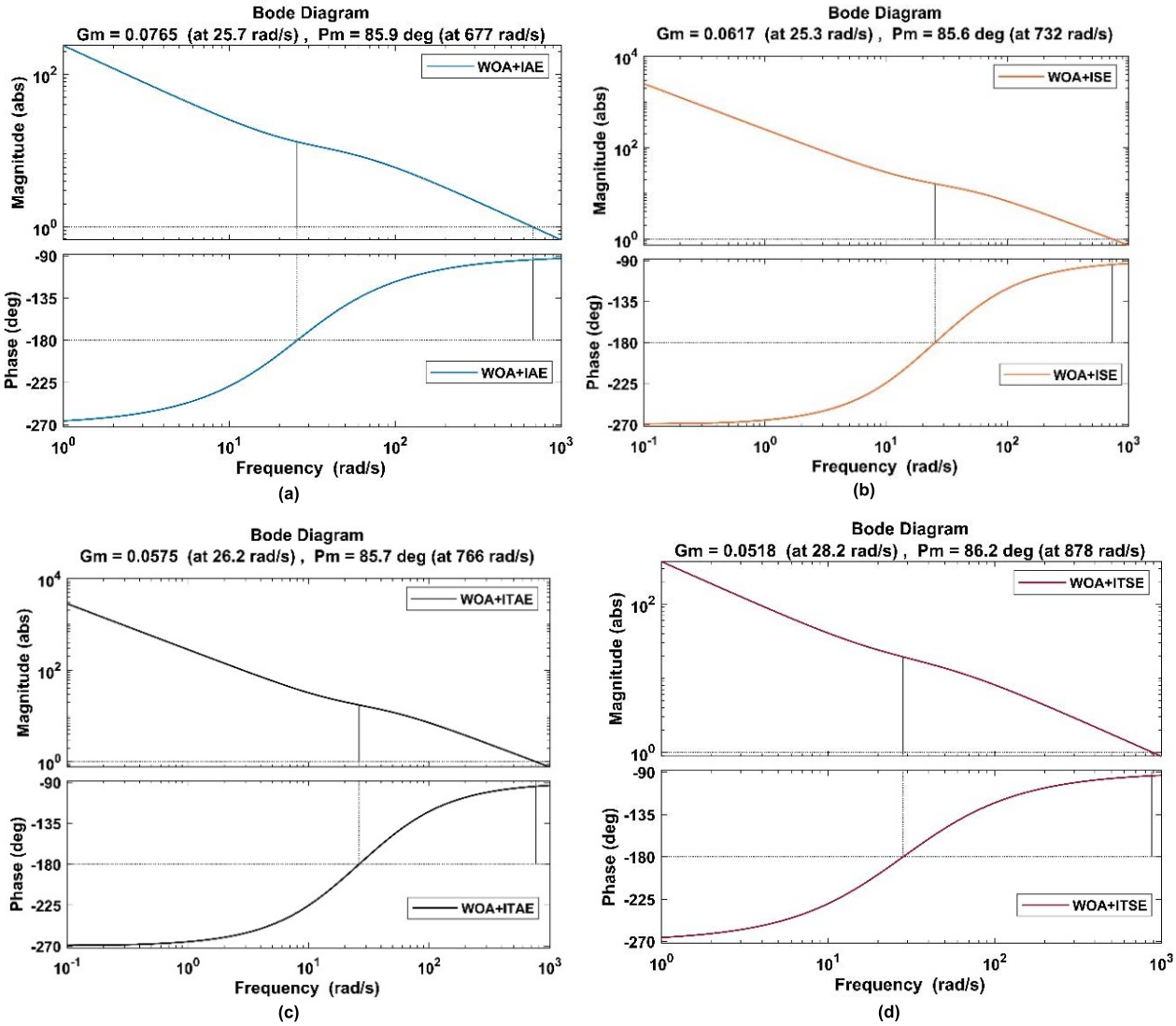


**FIGURE 18.** Bode plot of proposed closed-loop AMB system optimized by WOA with (a) IAE (b) ISE (c) ITAE and (d) ITSE objective functions.

**TABLE 11.** Data of statistical analysis on grey wolf optimization (GWO) algorithm.

| Sl. No. | Parameters | GWO-IAE | GWO -ISE | GWO - ITAE | GWO - ITSE |
|---|---|---|---|---|---|
| 1. | Mean | 1.00899040 | 1.00798204 | 0.50449280 | 0.50398608 |
| 2. | Standard Deviation | 2.8149097e-07 | 1.3417491e-07 | 2.9852563e-08 | 3.1435006e-08 |
| 3. | Variance | 7.9237169e-14 | 1.8002907e-14 | 8.91175562 e-16 | 9.8815963e-16 |
| 4. | Minimum value of objective function | 1.00899037 | 1.00798203 | 0.50449280 | 0.50398608 |
| 5. | Maximum value of objective function | 1.00899319 | 1.00798337 | 0.50449310 | 0.50398639 |
| 6. | Difference | 2.81490975 e-06 | 1.34174912 e-06 | 2.98525637 e-07 | 3.14380147 e-07 |

**TABLE 12.** Data of statistical analysis on wolf optimization algorithm (WOA).

| Sl. No. | Parameters | WOA-IAE | WOA -ISE | WOA - ITAE | WOA - ITSE |
|---|---|---|---|---|---|
| 1. | Mean | 1.00899363 | 1.00798830 | 0.50449443 | 0.50398937 |
| 2. | Standard Deviation | 1.99261336 e-08 | 9.96010808 e-08 | 4.36627848 e-09 | 1.63358529 e-08 |
| 3. | Variance | 3.97050802 e-16 | 9.92037530 e-15 | 1.90643877 e-17 | 2.66860090 e-16 |
| 4. | Minimum value of objective function | 1.00899363 | 1.00798828 | 0.50449443 | 0.50398937 |
| 5. | Maximum value of objective function | 1.00899383 | 1.00798928 | 0.50449447 | 0.50398954 |
| 6. | Difference | 1.99261336 e-07 | 9.96606502 e-07 | 4.36627848 e-08 | 1.63359131 e-07 |

Later in this manuscript, a comparison among the performance of these optimization techniques with different objective functions is examined based on statistical data, time-domain analysis, phase margin, and time taken in the execution of the algorithm.

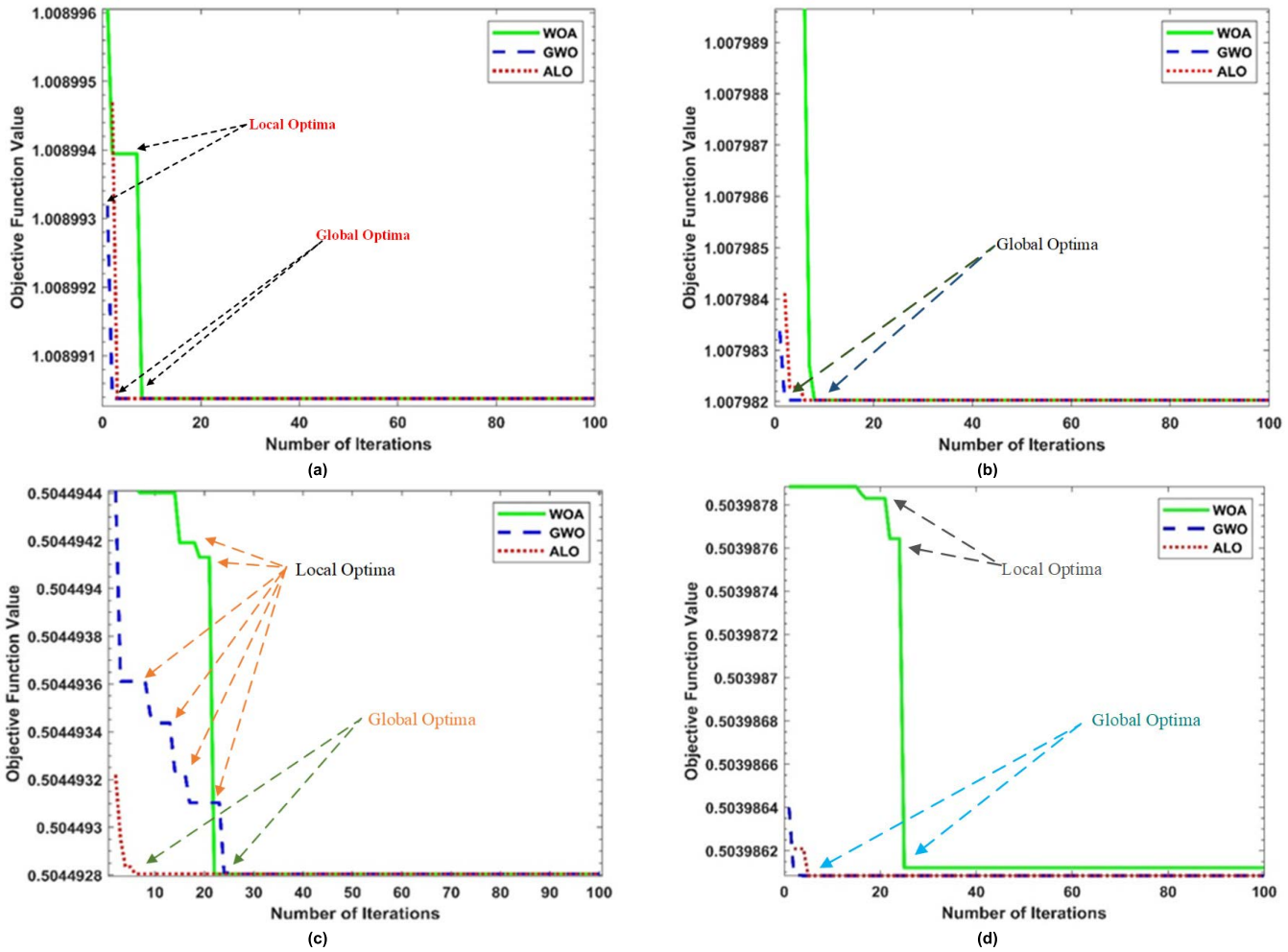


**FIGURE 19.** Performance of objective functions with ALO, GWO and WOA technique with (a) IAE, (b) ISE, (c) ITAE, and (d) ITSE, for 100 no. of iterations.

### *D. PERFORMANCE COMPARISON OF ALO, GWO, AND WOA ALGORITHMS WITH DIFFERENT OBJECTIVE FUNCTIONS*

Each optimization technique is executed with four different objective functions separately for $T$ number of iterations. Variations in the obtained value of an objective function concerning the number of iterations are observed and plotted as depicted in Figure 19 (when $T = 100$) and Figure 20(when $T = 500$)

*Case A*- when $T = 100$,

*Case B*- when $T = 500$,

Apart from the variation in objective function value concerning the increasing number of iterations, various statistical data have been observed like the mean of the objective function value over the number of iterations, standard deviation, variance, the minimum and maximum value of the objective function, the difference between the minimum and maximum value of objective functions. These data are used to perform a comparison among optimization techniques which is explained in the next part of this section.

#### 1) ON THE BASIS OF DATA OBTAINED FROM STATISTICAL ANALYSIS

Statistical analysis is a scientific approach that empowers us to expand our understanding of analyzing data and extract meaningful information from the available data [45]. In this manuscript, basic mathematical tools used for analyzing numerical data are- Mean, standard deviation, and variance. The value of these three statistical parameters is calculated for data obtained from the execution of optimization techniques. Realized value of statistical parameters for the different objective functions and optimization techniques is listed in Table 10- Table 12.

En masse, analyzing the data of Table 10-12, a comparison is observed as shown in Figure 21.

The significance of this comparison is to get a clear understanding of variations in parameters of statistical data. The first statistical parameter - The mean shows the final value of the objective function and from Figure 21 (a) it is evident that the IAE objective function gives the maximum value of the objective function followed by the ISE objective function.

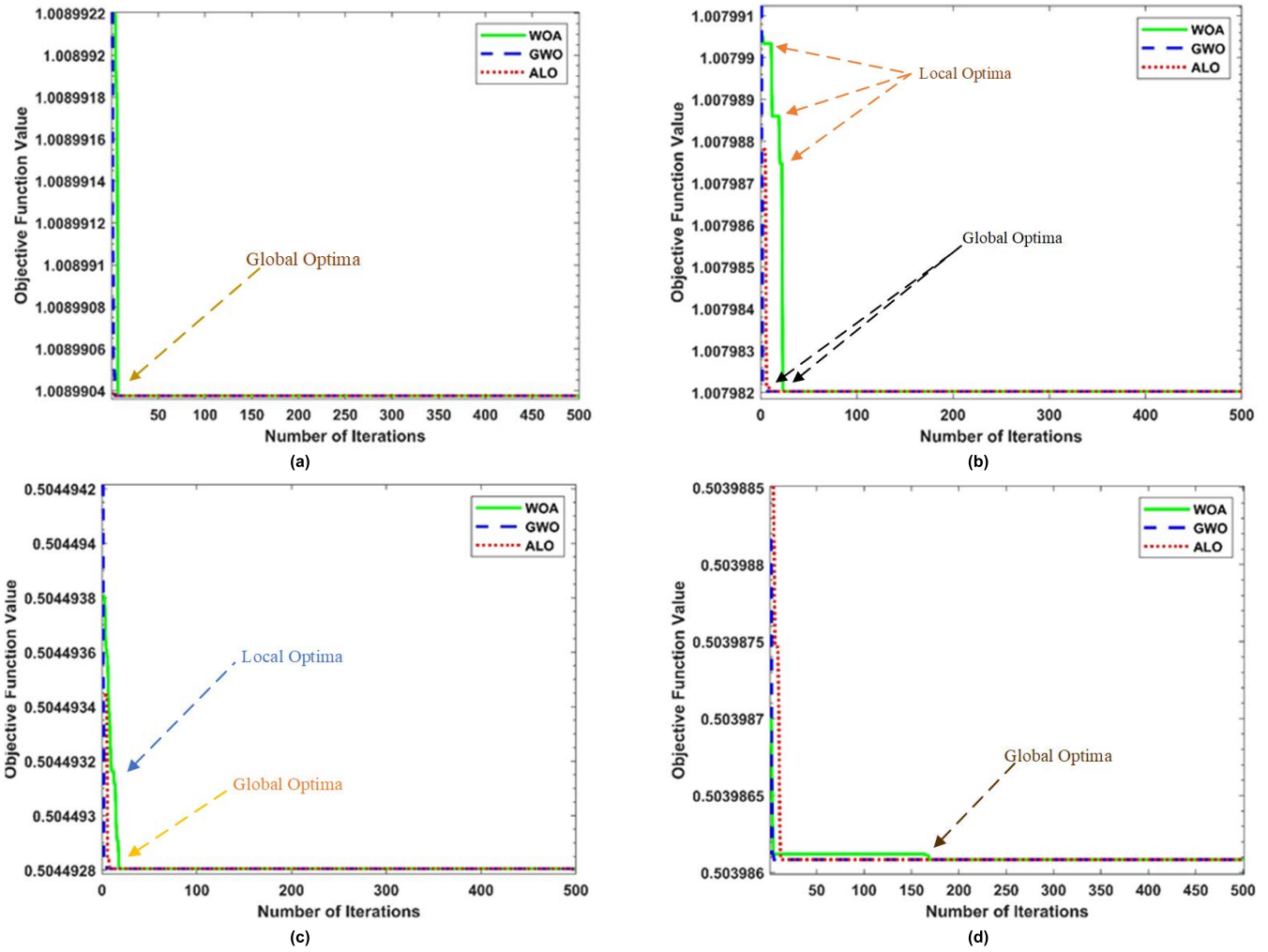


**FIGURE 20.** Performance of objective functions with ALO, GWO, and WOA technique with (a) IAE, (b) ISE, (c) ITAE, and (d) ITSE, for 500 no. of iterations.

On the contrary, with ITSE objective function optimization gets improved and the objective function value gets reduced to a minimum. The second best minimum value of the objective function is obtained by using ITAE objective function.

Next statistical parameter- Standard deviation represents a measurement of data dispersion regarding the mean. From the calculated data it is observable in Figure 21 (b) that the value of standard deviation is closer to zero therefore the data points are close to the mean. This explains that for most of the iterations objective function value is closer to the mean value. That's the reason for selecting the mean value as the final value of an objective function.

Variance indicated how much data in a set of data differ from one another. Mathematically, it is defined as the average of the squared differences from the Mean. Diverseness in observed data is depicted in Figure 21 (c).

### 2) ON THE BASIS OF DATA OBSERVED FROM TRANSIENT STATE ANALYSIS AND PHASE MARGIN

The main objective of this work is to make the proposed closed-loop system stable for a smooth and proper bearing operation. The performance of a closed-loop can be measured with the help of transient state analysis and comments on stability can be made by analyzing the phase margin of the system. The proposed system value of various transient state parameters like, peak overshoot, rise time, peak time, and settling time is listed in Table 3, Table 6, and Table 9 using these data, a comparison is observed and depicted in Figure 22.

The low value of peak overshoot results in less vibration in the system at a transient state which is an essential requirement for a steady bearing operation. So, the major challenge is in the selection of optimization techniques along with objective function. It is evident from Figure 22(a) that the ALO optimization technique with ITSE objective function (ALO-ITSE) shows a minimum overshoot of 6.07% followed by GWO-ITSE and WOA-ITSE with a value of 6.32% and 6.44% respectively. From the aspect of the objective function, the ITSE objective function shows a better transient state performance than other objective functions.

Another parameter that is required for the selection of optimization technique and objective function is the speed of response of the closed-loop system. Comment on the speed of

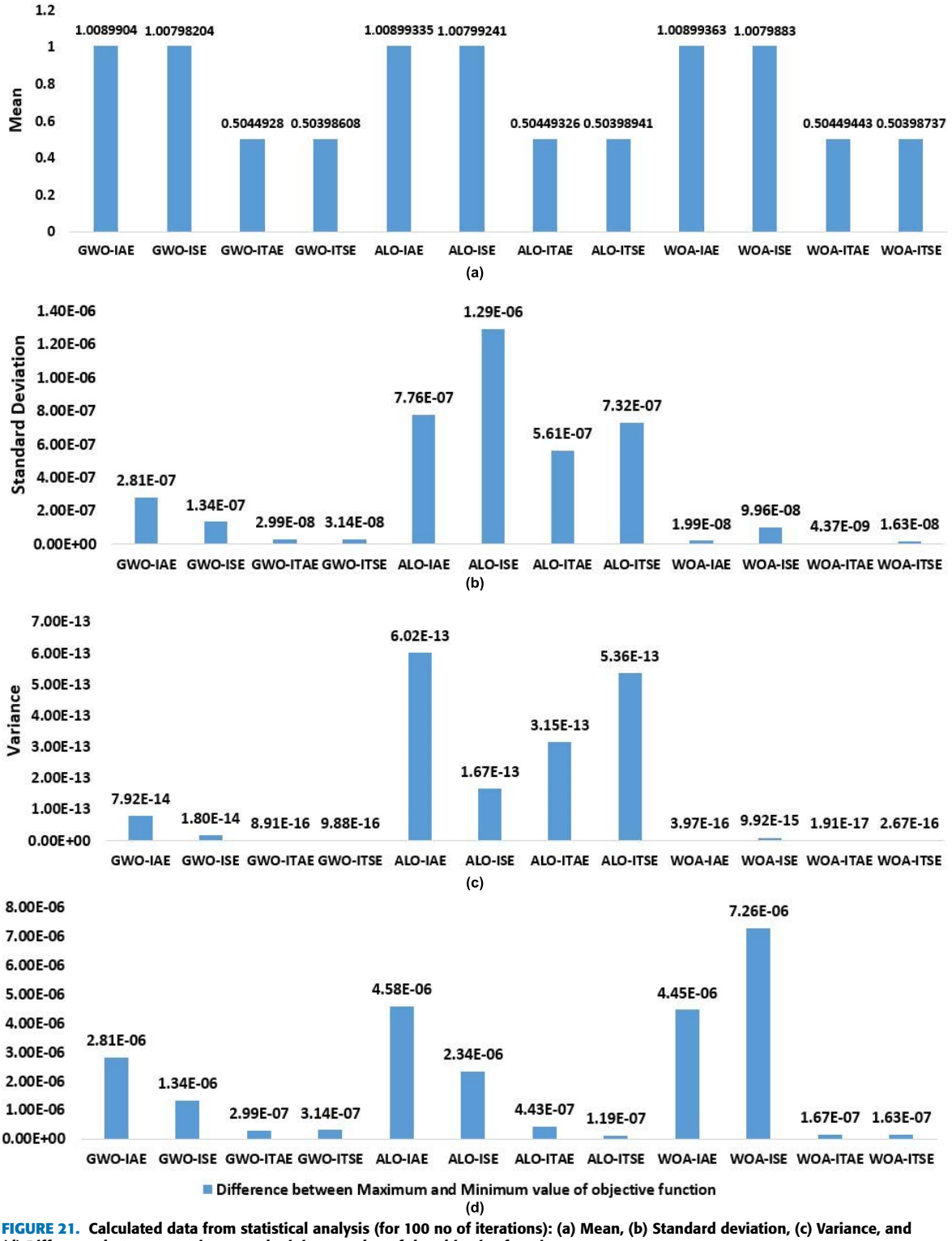


**FIGURE 21.** Calculated data from statistical analysis (for 100 no of iterations): (a) Mean, (b) Standard deviation, (c) Variance, and (d) Difference between maximum and minimum value of the objective function.

response of the closed-loop system can be made by observing the data of rising time, peak time, and settling time. For a sluggish response value of rising, peak and settling time is more and for a rapid response, these values should be as minimum as possible without disturbing the stability of the system. Readily, it is observable from Figure 22(b)- Figure 22(d) that the ITSE objective function shows a faster response as compared to other objective functions. From the perspective of optimization technique, ALO has a faster rise time and settling time followed by GWO and WOA. The most crucial

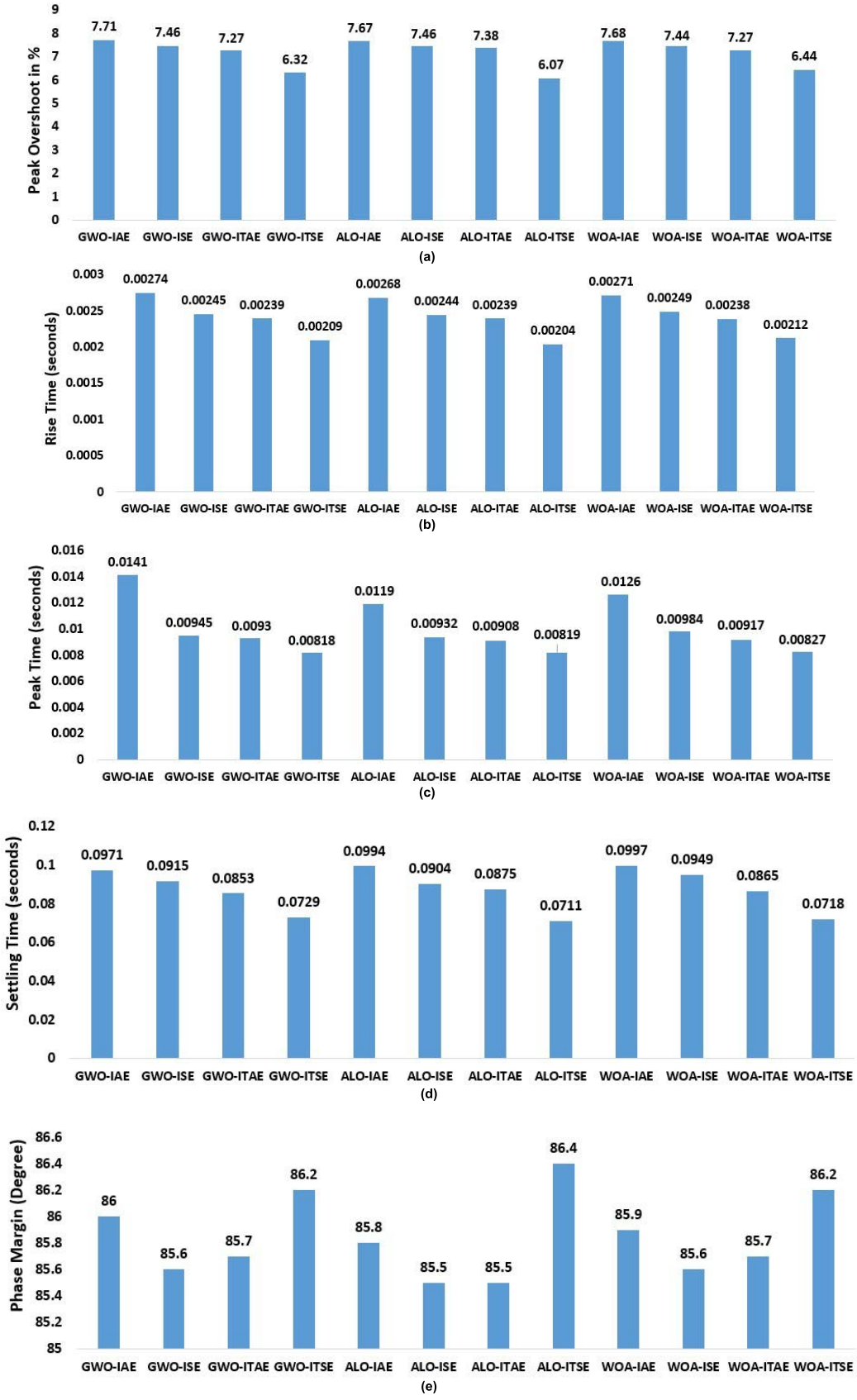


**FIGURE 22.** Observed data from time domain analysis: (a) Peak overshoot (%), (b) Peak time (in seconds), (c) Rise time (in seconds), (d) Settling time (in seconds) and (e) Phase Margin (in degree).

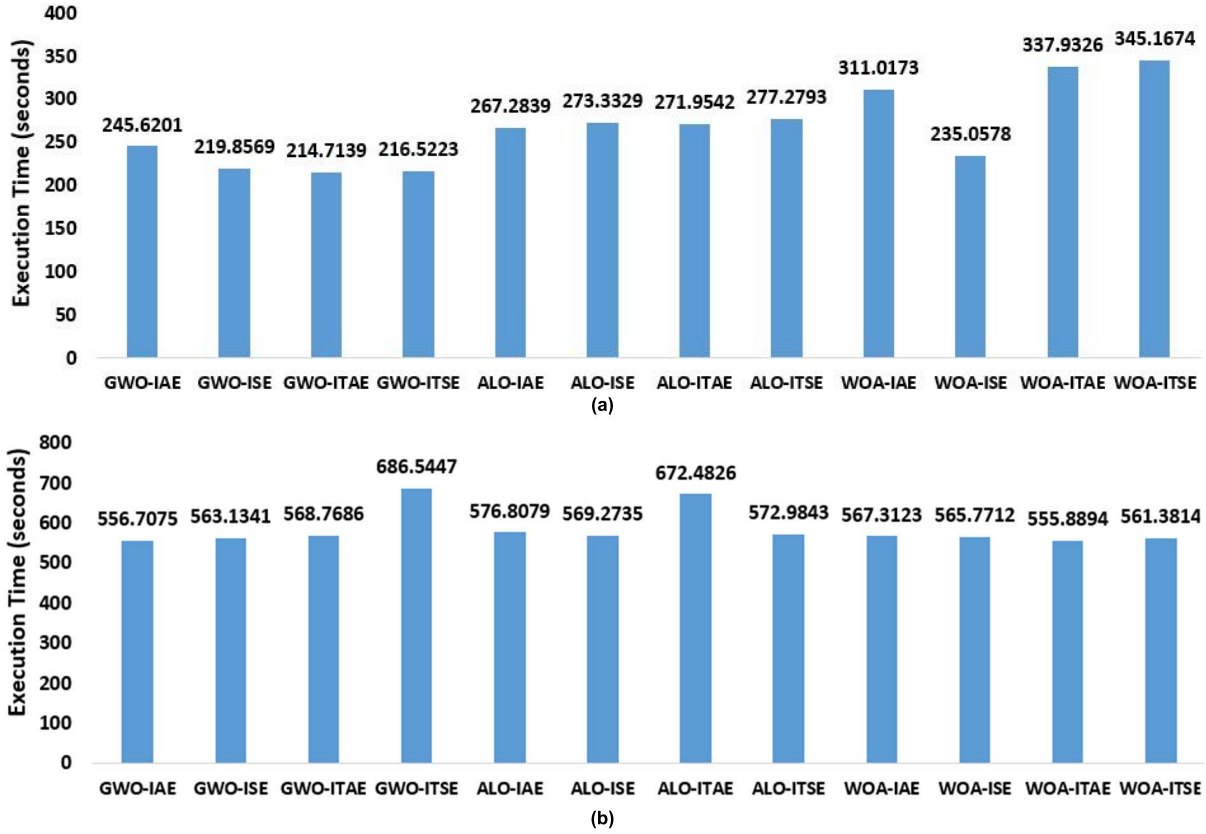


**FIGURE 23.** Algorithm execution time for (a) 100 iterations, (b) 500 number of iteration.

parameter in the selection of a controller for an unstable system is stability. It is the reason for the stable close loop operation of a system after then only transient state and steady-state analysis can be observed. The stability of a closed-loop system can be measured by measuring the phase margin of the system. Greater the phase margin greater the range of stability of the system. From Figure 22(e) it can be observed that among all, ALO-ITSE has the greatest value of phase margin of $86.4^0$ followed by GWO-ITSE and WOA-ITSE.

### 3) ON THE BASIS OF ALGORITHM EXECUTION TIME

The efficiency of an optimization algorithm depends on the number of computational resources used and the time taken by the algorithm to generate the desired outcome. Required mathematical resources for all three optimization techniques are almost observed. Therefore, the remaining parameter i.e., algorithm execution time, will need to calculate for realizing the performance of the optimization technique. For 100 number iterations ($T = 100$) and 500 iterations ($T = 500$), the algorithm execution time for all three optimization techniques is calculated as listed in Table 13. A comparison is carried out as depicted in Figure 23(a) for $T = 100$ and (b) for $T = 500$.

For $T = 100$, the minimum algorithm execution time is taken by the grey wolf optimization technique followed by ALO and then the WOA method. Whereas, the minimum average algorithm execution time for $T = 500$ is taken by the whale optimization algorithm followed by ALO and GWO methods.

**TABLE 13.** Execution time (in seconds) of fa, goa and abc algorithm with objective functions.

| Sl. No. | Algorithm | Objective functions | Algorithm execution time (in seconds) for $T$= 100 | Algorithm execution time (in seconds) for $T$= 500 |
|---|---|---|---|---|
| 1. | Ant lion optimization (ALO) | IAE | 267.2839 | 556.7075 |
| | | ISE | 273.3329 | 563.1341 |
| | | ITAE | 271.9542 | 568.7686 |
| | | ITSE | 277.2793 | 686.5447 |
| | | | | |
| 2. | Grey wolf optimization (GWO) | IAE | 245.6201 | 576.8079 |
| | | ISE | 219.8569 | 569.2735 |
| | | ITAE | 214.7139 | 672.4826 |
| | | ITSE | 216.5223 | 572.9843 |
| | | | | |
| 3. | Whale optimization algorithm (WOA) | IAE | 311.0173 | 567.3123 |
| | | ISE | 235.0578 | 565.7712 |
| | | ITAE | 337.9326 | 555.8894 |
| | | ITSE | 345.1674 | 561.3814 |

## V. CONCLUSION

In this manuscript, three different metaheuristic nature-inspired hunting-based optimization strategies- ALO, GWO,

and WOA, are implemented separately, to calculate the gain parameters of a PID controller for the proposed closed-loop AMB system. Execution of these algorithms is carried out on IAE, ISE, ITAE, and ITSE objective functions individually and their performance is statistically analyzed. Further, the action of the controller on the closed-loop is observed for each combination of algorithm-objective functions on the scale of step response analysis and bode plot. Using which transient state parameters and phase margin are calculated. Thoroughly comparing the obtained data it's realized that-

- Statistical analysis shows that algorithms with ITSE objective function have attained a minimum value compared to other objective functions.
- Also, transient state analysis data show that algorithms with ITSE objective function demonstrate a better closed-loop performance than other objective functions.
- Among these three optimization techniques, ALO with the ITSE objective function shows the best transient state characteristics with a lesser overshoot, faster response, and a wider phase margin.
- The time taken in execution of the algorithm is least using GWO-ITAE (for $T = 100$) and WOA-ITAE (for, $T = 500$).

This comparative study delivers a clear idea of the selection of optimization techniques along with objective functions from the perspective of their workability and performance, which will help in implementing them in a real-time situation.

## CONFLICT OF INTEREST

The authors declare no conflicts of interest to disclose.

## REFERENCES

[1] G. Schweitzer and E. H. Maslen, *Magnetic Bearings: Theory, Design, and Application to Rotating Machinery*. Berlin, Germany: Springer, 2009.
[2] G. Schweitzer, "Active magnetic bearings-chances and limitations," in *Proc. 6th Int. Conf. Rotor Dyn.*, 2002, pp. 1–14.
[3] H. Bangcheng, Z. Shiqiang, W. Xi, and Y. Qian, "Integral design and analysis of passive magnetic bearing and active radial magnetic bearing for agile satellite application," *IEEE Trans. Magn.*, vol. 48, no. 6, pp. 1959–1966, Jun. 2011.
[4] A. Smirnov, N. Uzhegov, T. Sillanpää, J. Pyrhönen, and O. Pyrhönen, "High-speed electrical machine with active magnetic bearing system optimization," *IEEE Trans. Ind. Electron.*, vol. 64, no. 12, pp. 9876–9885, Dec. 2017.
[5] X. Li, A. Palazzolo, and Z. Wang, "A combination 5-DOF active magnetic bearing for energy storage flywheels," *IEEE Trans. Transport. Electrific.*, vol. 7, no. 4, pp. 2344–2355, Dec. 2021, doi: 10.1109/TTE.2021.3079402.
[6] T. Soni, J. K. Dutt, and A. S. Das, "Magnetic bearings for marine rotor systems—Effect of standard ship maneuver," *IEEE Trans. Ind. Electron.*, vol. 68, no. 2, pp. 1055–1064, Feb. 2021, doi: 10.1109/TIE.2020.2967664.
[7] N. Uzhegov, A. Smirnov, C. H. Park, J. H. Ahn, J. Heikkinen, and J. Pyrhönen, "Design aspects of high-speed electrical machines with active magnetic bearings for compressor applications," *IEEE Trans. Ind. Electron.*, vol. 64, no. 11, pp. 8427–8436, Nov. 2017, doi: 10.1109/TIE.2017.2698408.
[8] T. Soni, J. K. Dutt, and A. S. Das, "Parametric stability analysis of active magnetic bearing supported rotor system with a novel control law subject to periodic base motion," *IEEE Trans. Ind. Electron.*, vol. 67, no. 2, pp. 1160–1170, Feb. 2020, doi: 10.1109/TIE.2019.2898604.
[9] Y. Xu, Q. Shen, Y. Zhang, J. Zhou, and C. Jin, "Dynamic modeling of the active magnetic bearing system operating in base motion condition," *IEEE Access*, vol. 8, pp. 166003–166013, 2020, doi: 10.1109/ACCESS.2020.3022996.
[10] G.-P. Ren, Z. Chen, H.-T. Zhang, Y. Wu, H. Meng, D. Wu, and H. Ding, "Design of interval type-2 fuzzy controllers for active magnetic bearing systems," *IEEE/ASME Trans. Mechatronics*, vol. 25, no. 5, pp. 2449–2459, Oct. 2020.
[11] X. Yao, Z. Chen, and Y. Jiao, "A dual-loop control approach of active magnetic bearing system for rotor tracking control," *IEEE Access*, vol. 7, pp. 121760–121768, 2019, doi: 10.1109/ACCESS.2019.2937191.
[12] A. Heya, K. Hirata, N. Niguchi, and A. Nakajima, "Triaxial active control magnetic bearing with asymmetric structure," *IEEE Trans. Ind. Appl.*, vol. 57, no. 5, pp. 4675–4685, Sep. 2021, doi: 10.1109/TIA.2021.3089557.
[13] S.-L. Chen, S.-Y. Lin, and C.-S. Toh, "Adaptive unbalance compensation for a three-pole active magnetic bearing system," *IEEE Trans. Ind. Electron.*, vol. 67, no. 3, pp. 2097–2106, Mar. 2020, doi: 10.1109/TIE.2019.2903747.
[14] S. Saha, S. M. Amrr, M. U. Nabi, and A. Iqbal, "Reduced order modeling and sliding mode control of active magnetic bearing," *IEEE Access*, vol. 7, pp. 113324–113334, 2019, doi: 10.1109/ACCESS.2019.2935541.
[15] S. Wang, H. Zhu, M. Wu, and W. Zhang, "Active disturbance rejection decoupling control for three-degree-of-freedom six-pole active magnetic bearing based on BP neural network," *IEEE Trans. Appl. Supercond.*, vol. 30, no. 4, pp. 1–5, Jun. 2020, doi: 10.1109/TASC.2020.2990794.
[16] H. S. Zad, T. I. Khan, and I. Lazoglu, "Design and adaptive sliding-mode control of hybrid magnetic bearings," *IEEE Trans. Ind. Electron.*, vol. 65, no. 3, pp. 2537–2547, Mar. 2018, doi: 10.1109/TIE.2017.2739682.
[17] S. Zhang, J. Zhou, H. Wu, and Y. Zhang, "Dynamic analysis of active magnetic bearing rotor system considering Alford force," *J. Vib. Eng. Technol.*, vol. 9, no. 6, pp. 1147–1154, Sep. 2021, doi: 10.1007/s42417-021-00287-w.
[18] S. Debnath and P. K. Biswas, "Advanced magnetic bearing device for high-speed applications with an I-type electromagnet," *Electr. Power Compon. Syst.*, vol. 48, nos. 16–17, pp. 1862–1874, 2021.
[19] C. Wei and D. Soffker, "Optimization strategy for PID-controller design of AMB rotor systems," *IEEE Trans. Control Syst. Technol.*, vol. 24, no. 3, pp. 788–803, May 2016, doi: 10.1109/TCST.2015.2476780.
[20] H. Gao, X. Meng, and K. Qian, "The impact analysis of beating vibration for active magnetic bearing," *IEEE Access*, vol. 7, pp. 134104–134112, 2019, doi: 10.1109/ACCESS.2019.2932723.
[21] J. Sun, H. Zhou, X. Ma, and Z. Ju, "Study on PID tuning strategy based on dynamic stiffness for radial active magnetic bearing," *ISA Trans.*, vol. 80, pp. 458–474, Sep. 2018, doi: 10.1016/j.isatra.2018.07.036.
[22] A. Dhyani, M. K. Panda, and B. Jha, "Moth-flame optimization-based fuzzy-PID controller for optimal control of active magnetic bearing system," *Iranian J. Sci. Technol., Trans. Electr. Eng.*, vol. 42, no. 4, pp. 451–463, Dec. 2018.
[23] Y. Liu, S. Ming, S. Zhao, J. Han, and Y. Ma, "Research on automatic balance control of active magnetic bearing-rigid rotor system," *Shock Vib.*, vol. 2019, pp. 1–13, Apr. 2019.
[24] A. Slowik and K. Cpalka, "Hybrid approaches to nature-inspired population-based intelligent optimization for industrial applications," *IEEE Trans. Ind. Informat.*, vol. 18, no. 1, pp. 546–558, Jan. 2022, doi: 10.1109/TII.2021.3067719.
[25] D. H. Wolper and W. G. Macready, "No free lunch theorems for optimization," *IEEE Trans. Evol. Comput.*, vol. 1, no. 1, pp. 67–82, Apr. 1997, doi: 10.1109/4235.585893.
[26] S. Debnath and P. K. Biswas, "Design, analysis, and testing of I-type electromagnetic actuator used in single-coil active magnetic bearing," *Electr. Eng.*, vol. 103, no. 1, pp. 183–194, Feb. 2021, doi: 10.1007/s00202-020-01071-x.
[27] D. Yang, X. Gao, E. Cui, and Z. Ma, "State-constraints adaptive backstepping control for active magnetic bearings with parameters nonstationarities and uncertainties," *IEEE Trans. Ind. Electron.*, vol. 68, no. 10, pp. 9822–9831, Oct. 2020.
[28] Y. B. Zheng, N. Mo, Y. Zhou, and Z. Shi, "Unbalance compensation and automatic balance of active magnetic bearing rotor system by using iterative learning control," *IEEE Access*, vol. 7, pp. 122613–122625, 2019.
[29] Y. He, X. He, J. Ma, and Y. Fang, "Optimization research on a switching power amplifier and a current control strategy of active magnetic bearing," *IEEE Access*, vol. 8, pp. 34833–34841, 2020, doi: 10.1109/ACCESS.2020.2974765.
[30] S. Mirjalili, "The ant lion optimizer," *Adv. Eng. Softw.*, vol. 83, pp. 80–98, May 2015.
[31] A. S. Assiri, A. G. Hussien, and M. Amin, "Ant lion optimization: Variants, hybrids, and applications," *IEEE Access*, vol. 8, pp. 77746–77764, 2020.

[32] L. Abualigah, M. Shehab, M. Alshinwan, S. Mirjalili, and M. A. Elaziz, "Ant lion optimizer: A comprehensive survey of its variants and applications," *Arch. Comput. Methods Eng.*, vol. 28, no. 3, pp. 1397–1416, May 2021.
[33] A. Y. Hatata and A. A. Hafez, "Ant lion optimizer versus particle swarm and artificial immune system for economical and eco-friendly power system operation," *Int. Trans. Electr. Energy Syst.*, vol. 29, no. 4, p. e2803, Apr. 2019.
[34] S. Mirjalili, S. M. Mirjalili, and A. Lewis, "Grey wolf optimizer," *Adv. Eng. Softw.*, vol. 69, pp. 46–61, Mar. 2014, doi: 10.1016/j.advengsoft.2013.12.007.
[35] X. Sun, Z. Jin, Y. Cai, Z. Yang, and L. Chen, "Grey wolf optimization algorithm based state feedback control for a bearingless permanent magnet synchronous machine," *IEEE Trans. Power Electron.*, vol. 35, no. 12, pp. 13631–13640, Dec. 2020.
[36] X. Sun, C. Hu, G. Lei, Y. Guo, and J. Zhu, "State feedback control for a PM hub motor based on gray wolf optimization algorithm," *IEEE Trans. Power Electron.*, vol. 35, no. 1, pp. 1136–1146, Jan. 2019.
[37] X. Li and K. M. Luk, "The grey wolf optimizer and its applications in electromagnetics," *IEEE Trans. Antennas Propag.*, vol. 68, no. 3, pp. 2186–2197, Mar. 2019.
[38] J. C. Zhang, X. S. Wang, and L. Y. Ma, "An optimal power allocation scheme of microgrid using grey wolf optimizer," *IEEE Access*, vol. 7, pp. 137608–137619, 2019.
[39] S. Mirjalili and A. Lewis, "The whale optimization algorithm," *Adv. Eng. Softw.*, vol. 95, pp. 51–67, May 2016.
[40] P. R. Hof and E. Van Der Gucht, "Structure of the cerebral cortex of the humpback whale, *Megaptera novaeangliae* (Cetacea, Mysticeti, Balaenopteridae)," *Anatomical Rec., Adv. Integrative Anatomy Evol. Biol.*, vol. 290, no. 1, pp. 1–31, Jan. 2007, doi: 10.1002/ar.20407.
[41] S. Mirjalili, S. M. Mirjalili, S. Saremi, and S. Mirjalili, "Whale optimization algorithm: Theory, literature review, and application in designing photonic crystal filters," *Nature-Inspired Optimizers*, vol. 811, pp. 219–238, Feb. 2020.
[42] M. H. Qais, H. M. Hasanien, and S. Alghuwainem, "Whale optimization algorithm-based sugeno fuzzy logic controller for fault ride-through improvement of grid-connected variable speed wind generators," *Eng. Appl. Artif. Intell.*, vol. 87, Jan. 2020, Art. no. 103328.
[43] P. D. P. Reddy, V. C. V. Reddy, and T. G. Manohar, "Optimal renewable resources placement in distribution networks by combined power loss index and whale optimization algorithms," *J. Elect. Syst. Inf. Technol.*, vol. 5, pp. 175–191, Sep. 2018.
[44] M. S. Tavazoei, "Notes on integral performance indices in fractional-order control systems," *J. Process. Control*, vol. 20, no. 3, pp. 285–291, Mar. 2010.
[45] D. I. Mattos, J. Bosch, and H. H. Olsson, "Statistical models for the analysis of optimization algorithms with benchmark functions," *IEEE Trans. Evol. Comput.*, vol. 25, no. 6, pp. 1163–1177, Dec. 2021, doi: 10.1109/TEVC.2021.3081167.

**SURAJ GUPTA** received the B.Tech. degree from Uttar Pradesh Technical University, India, in 2013, and the M.Tech. degree in power electronics and drives from the National Institute of Technology Mizoram, Aizawl, India, in 2018, where he is currently pursuing the Ph.D. degree with the Department of Electrical and Electronics Engineering.

**PABITRA KUMAR BISWAS** (Member, IEEE) received the B.Tech. degree from Asansol Engineering College, West Bengal University of Technology (WBUT), West Bengal, India, the M.E. degree in electrical and electronics engineering (power electronics and drives) from Bengal Engineering and Science University, West Bengal, in 2007, and the Ph.D. degree in electrical engineering from the National Institute of Technology, Durgapur, India, in 2013. He was the HoD of the Department of Electrical and Electronics Engineering (EEE), from February 2015 to August 2019. He is currently working as an Assistant Professor and the HoD in electrical and electronics engineering with the National Institute of Technology Mizoram, India. He has published a numbers of research papers in national/international conference and records/journals. He has a book and more than six book chapters and filed three patents. He has completed one DST-SERB Project. He has about 14 years of academic as well as research experience. He has guided five Ph.D. students, more than ten M.Tech. students, and more than ten are pursuing their research at present. He has successfully organized a GIAN course, two short term course, and a FDP (ATAL). His research interests include electromagnetic levitation systems, active magnetic bearing, power electronics converters, PMSM and BLDC motor drives, electric vehicles, and renewable energy. He is a member of the Institute of Engineers and International Association of Engineers. He is also a Fellow Membership (FSASS) of SAS Society. He has received the Best Paper Award and the Best Researcher Award (International Scientist Awards on Engineering, Science and Medicine). He has reviewed papers in reputed international conference and journals.

**THANIKANTI SUDHAKAR BABU** (Senior Member, IEEE) received the B.Tech. degree from Jawaharlal Nehru Technological University, Anantapur, India, in 2009, the M.Tech. degree in power electronics and industrial drives from Anna University, Chennai, India, in 2011, and the Ph.D. degree from VIT University, Vellore, India, in 2017.

He had completed the Postdoctoral Researcher Fellowship from the Institute of Power Engineering, Universiti Tenaga Nasional (UNITEN), Malaysia. He was an Assistant Professor at the School of Electrical Engineering, VIT University. He is currently an Associate Professor with the Department of Electrical Engineering, Chaitanya Bharathi Institute of Technology (CBIT), Hyderabad, India. He has published more than 115 research articles in various renowned international journals. His research interests include design and implementation of solar PV systems, renewable energy resources, power management for hybrid energy systems, storage systems, fuel cell technologies, electric vehicles, and smart grids.

Dr. Sudhakar Babu is an Associate Editor of *IET Renewable Power Generation* (RPG), IEEE Access, *International Transactions on Electrical Energy Systems* (ITEES) (Willey), and *Frontiers in Energy Research* and a Section Editor of *Energies and Sustainability* (MDPI). He is a reviewer of various reputed journals.

**HASSAN HAES ALHELOU** (Senior Member, IEEE) was a Ph.D. Researcher at the Isfahan University of Technology (IUT), Isfahan, Iran. He is currently a Faculty Member at Tisheen University, Latakia, Syria. He has published more than 30 research papers in the high quality peer-reviewed journals and international conferences. He has also performed more than 160 reviews for high prestigious journals, including IEEE Transactions on Industrial Informatics, IEEE Transactions on Industrial Electronics, *Energy Conversion and Management*, *Applied Energy*, and *International Journal of Electrical Power & Energy Systems*. He has participated in more than 15 industrial projects. His major research interests include power systems, power system dynamics, power system operation and control, dynamic state estimation, frequency control, smart grids, microgrids, demand response, load shedding, and power system protection. In 2018 and 2019, he was included in the Publons list of the top 1% best reviewer and researchers in the field of engineering. He was a recipient of the Outstanding Reviewer Award from *Energy Conversion and Management* journal, in 2016, *ISA Transactions* journal, in 2018, *Applied Energy* journal, in 2019, and many other Awards. He was also a recipient of the Best Young Researcher Award in the Arab Student Forum Creative among 61 researchers from 16 countries at Alexandria University, Egypt, in 2011.